Electronic Supplementary Material (ESI) for Organic Chemistry Frontiers.

Electronic Supporting Information

Discovery and characterization of a novel sub-group of UbiA-type terpene cyclases with a distinct motif I

Pan Luo,[a*] Jian-Ming Lv,[a*] Yan-Feng Xie,[a] Liang-Yan Xiao,[a] Sheng-Ying Qin,[b] Guo-Dong Chen,[a] Xiao-Zhou Luo,[c] Dan Hu,[a,c#] Hao Gao[a#]

[a] Institute of Traditional Chinese Medicine & Natural Products, College of Pharmacy / Guangdong Province Key Laboratory of Pharmacodynamic Constituents of TCM and New Drugs Research / International Cooperative Laboratory of Traditional Chinese Medicine Modernization and Innovative Drug Development of Ministry of Education (MOE) of China, Jinan University, Guangzhou 510632, China

[b] Clinical Experimental Center, First Affiliated Hospital of Jinan University, Guangzhou 510630, China

[c] Shenzhen Institute of Synthetic Biology, Shenzhen Institute of Advanced Technology, Chinese Academy of Sciences, Shenzhen 518055, China.

Table of contents

Supplementary Methods

General materials and experimental procedures

All the chemicals were purchased from Oceanpak Alexative Chemical Co., Ltd. (Gothenburg, Sweden) or Fine Chemical Co., Ltd. (Tianjin, China). The biochemical reagents and kits used in this work were purchased from TaKaRa Bio Inc. (Dalian, China), Thermo Fisher Scientific Inc. (Shenzhen, China), or Sangon Biotech Co., Ltd. (Shanghai, China), unless noted otherwise. Primer synthesis was performed by Sangon Biotech Co., Ltd. (Shanghai, China) or Tsingke Biotech Co., Ltd. (Beijing, China). PCR was carried out using a Mastercycler® nexus gradient (Eppendorf, Hamburg, Germany) or an A100 Thermal cycler (LongGene, Hangzhou, China).

Optical rotations were measured on the JASCO P2000 digital polarimeter from JASCO International Co., Ltd. (Tokyo, Japan). NMR spectra were recorded with the Bruker AV 400/600 spectrometers (Faellanden, Switzerland) using the solvent signals ($CDCl_3$: δ_H 7.26/δ_C 77.0) as the reference. The HRESIMS data were obtained from SYNAPT G2 high definition mass spectrometer (Waters, Milford, USA). The semi-preparative HPLC was performed on an Ultimate 3000 HPLC system (Dionex) with a YMC Pack ODS-A column (10.0 mm i.d. × 250 mm, 5 μm). The chiral chromatography was carried out using a Phenomenex i-Cellulose-5 column (250 × 4.6 mm, 5 μm) from Phenomenex Scientific Instrument Co., Ltd. (Guangzhou, China). The silica gel column chromatography was performed with silica gel (300–400 mesh, Haiyang Chemical Co., Ltd., Qingdao, China).

Strains and media

The engineered *Saccharomyces cerevisiae* CEN.PK2-1C (erg9::KanMX/CTR3p-*ERG9*; leu2-3_112::His3MX6/GAL1p-*ERG19*/GAL10p-*ERG8*; ura3-52::GAL1p-*EfMvaS(A110G)*-CYC1t/GAL10p-*EfMvaE*-ADH1t; his3Δ1::hphMX4/GAL1p-*ERG12*/GAL10p-*IDI1*; 1014a::GAL1p-*Erg20*) was used for heterologous expression of sesquiterpene synthase genes. These exogenous genes were driven by the *GAL1* promoter in the synthetic galactose minimal medium lacking uracil (SG–URA) with addition of 37.45 mg/L $CuSO_4 \cdot 5H_2O$. *Escherichia coli* DH5α transformants carrying recombinant plasmids were grown in LB medium with 100 mg/L ampicillin.

Gene cloning and plasmid construction

The genes were either amplified from genomic DNA or artificially synthesized by Sangon

Biotech Co., Ltd. For expression in *S. cerevisiae*, these resulted DNA fragments were reassembled through the overlap extension PCR method to remove introns. And then the intron-free genes were respectively cloned into the linearized vector pESC-URA using the ClonExpress® II One Step Cloning Kit (Vazyme, Nanjing, China). For site-directed mutagenesis, the parental plasmid was amplified through PCR to afford the mutant vector, and then the parental plasmid was digested by the methylation-sensitive restriction enzyme DpnI.

Transformation of *S. cerevisiae*

Preparation and transformation of competent yeast cells were performed according to the Frozen-EZ Yeast Transformation II™ kit (Zymo Research Co., Ltd., Beijing, China) user manual. Yeast cells were cultured at 30 °C in 10 mL YPD broth (0.0075% L-adenine, 1% yeast extract, 2% peptone, 2% dextrose) until the OD_{600} value reached 0.8–1.0. And the pellet was collected through centrifugation at 500 g for 4 min, and washed once with 10 mL EZ 1 solution. Then the pellet was resuspended in 1 mL EZ 2 solution. Finally, the resulting competent cells were stored at –80 °C for future use. For yeast transformation, 50 μL of competent cells were thoroughly mixed with 0.2-1.0 μg DNA (< 5 μL) and 500 μL EZ 3 solution. After incubated at 30 °C for 45 min, the mixture was spreaded on the solid synthetic dextrose minimal medium without uracil (SD–URA) to screen transformants.

Analysis of metabolites from *S. cerevisiae* transformants

The yeast transformant was inoculated into 10 mL SD–URA medium and cultured at 30 °C and 220 rpm for 1 day as the seed broth. Then the broth was transferred into 100 mL SG–URA medium with addition of Cu^{2+}. After growing for 5 days, the pellet was harvested by centrifugation and extracted with 95% ethanol through ultrasound assisted extraction. The crude extract was concentrated under reduced pressure, and then partitioned with hexane-water (1/1, v/v) for GC-MS analysis, or resuspended in methanol for HPLC analysis.

GC-MS analysis was performed on Agilent Technologies 7890B GC System coupled with 5977B MSD using an HP-5MS column (30 m, 0.25 mm i. d., 0.50 μm film). The temperature of the ionization chamber was 230 °C, and the electron impact ionization voltage was 70 eV. The oven temperature initially kept at 50 °C for 3 min, then increased to 70 °C at a rate of 20 °C/min and held for 1 min, followed by a second ramp from 70 °C to 300 °C at a rate of 15 °C/min and holding for 3 min. Helium was used as carrier gas at the rate of 1 mL/min.

HPLC profile was detected on an Ultimate 3000 HPLC system (Dionex) using CH_3CN and H_2O as mobile phases. For analysis of metabolites from transformants containing *fusTC1* or *staTC1*, Phenomenex i-Cellulose-5 was used, and the sample was analyzed with isocratic elution of 45% CH_3CN for 60 min at 0.8 mL/min. The metabolites of transformants harboring mutated *staTC1* were detected using a COSMOSIL $3C_{18}$-EB column (4.6 mm i.d. × 150 mm, 3 μm) with a linear gradient elution of 50%–100% CH_3CN in 15 min followed by 100% CH_3CN for 45 min at 0.8 mL/min.

Preparation of microsomal fraction from the *S. cerevisiae* transformant

The *S. cerevisiae* transformant was grown in 100 mL SD–URA medium at 220 rpm and 30 °C for 2 days. After centrifugation at 5000 g for 10 min, the cells were collected and transferred into 100 mL YPG medium (10 g/L yeast extract, 20 g/L peptone, 20 g/L galactose, 0.1 g/L adenine) and cultured for 2 days. Subsequently, the cells were collected by centrifugation at 8000 g and 4 °C for 10 min and then washed four times with Buffer A (0.1 M KCl, 1.0 mM EDTA, 50 mM Tris-HCl, pH 7.5). The cells were then resuspended in Buffer B (0.6 M sorbitol, 0.1 M KCl, 1.0 mM EDTA, 2.0 mM DTT, 1.0 mM PMSF, 50 mM Tris-HCl, pH 7.5) and lysed by a cell disruptor (Constant Systems, United Kingdom). The lysate was centrifuged at 8000 g and 4 °C for 10 min, and the supernatant was further fractionated by ultracentrifugation at 100000 g and 4 °C for 1.5 h. The microsomal pellet was resuspended in 1 mL of Buffer C (20% glycerol, 1.0 mM EDTA, 1.0 mM DTT, 50 mM Tris-HCl, pH 7.5) and used for *in vitro* assay.

In vitro enzymatic reaction

To analyze the function of FusTC1 *in vitro*, the reaction mixture containing 300 μL microsomal fraction of the *S. cerevisiae* transformant harboring *fusTC1* and 3 μL FPP (1 mg/mL) was incubated at 30 °C overnight with addition of 8 μL EDTA (100 mM) or 15 μL $MgCl_2$ (100 mM). The microsomal fraction of the parent host was used as the control. After that, the reaction mixture was extracted three times with ethyl acetate and analyzed by GC-MS.

Purification procedure for metabolites

The *S. cerevisiae* transformant was cultured in SG–URA medium with addition of Cu^{2+} at 30 °C for 5 days. The cells were harvested by centrifugation at 8000 g for 30 min and then extracted with 95% ethanol for three times through ultrasound assisted extraction. And the culture medium was extracted with ethyl acetate. Subsequently, the extract of cells and culture medium was combined, and then concentrated under reduced pressure.

Purification process for **1** and **2**

The cells and culture medium extract from 5 L culture of *S. cerevisiae* harboring *fusTC1* was subjected to silica gel column chromatography with stepwise elution of cyclohexane and ethyl acetate (100:0 and 100:1, v/v) to yield fractions A and B in order. Fraction B (about 450 mg) was purified through semi-preparative HPLC (YMC-Pack ODS-A column, 2.0 mL/min) with 80% CH_3CN-H_2O to yield the mixture of **1** and **2**, which was further separated by a chiral HPLC column [Phenomenex i-Cellulose-5 (250 × 4.6 mm, 5 μm)] with isocratic elution of 45% CH_3CN-H_2O at the rate of 0.8 mL/min to yield **1** (10.0 mg) and **2** (11.0 mg). In addition, we also isolated **1** from the *S. cerevisiae* transformant harboring *staTC1*, and **2** from two other *S. cerevisiae* transformants harboring *staTC6* or *myrTC3*, respectively.

Purification process for **3**

The cells and culture medium extract (4.7 g) from 6 L culture of *S. cerevisiae* harboring *staTC2* was subjected to silica gel column chromatography with stepwise elution of cyclohexane and ethyl acetate (100:0 and 100:1, v/v) to afford fractions A and B. Fraction B (about 500 mg) was separated by semi-preparative HPLC (YMC-Pack ODS-A column, 2.0 mL/min) with 80% CH_3CN-H_2O to yield **3** (3.6 mg).

Purification process for **4**

The cells and culture medium extract (2.7 g) from 3 L culture of *S. cerevisiae* harboring *talTC2* was subjected to silica gel column chromatography with elution of cyclohexane to obtain about 140 mg fraction. This fraction was then purified by semi-preparative HPLC (YMC-Pack ODS-A column, 2.0 mL/min) with 95% MeOH-THF to yield **4** (40.0 mg).

Purification process for **5**

The cells and culture medium extract (1.7 g) from 3 L culture of *S. cerevisiae* harboring *myrTC4* was subjected to silica gel column chromatography by eluting with cyclohexane to obtain about 100 mg fraction. This fraction was then separated by semi-preparative HPLC (YMC-Pack ODS-A column, 2.0 mL/min) with 95% MeOH-THF to yield **5** (13.0 mg).

Purification process for **6**

The cells and culture medium extract (1.3 g) from 4 L culture of *S. cerevisiae* harboring *staTC5* was loaded onto a silica gel column and eluted with cyclohexane to obtain about 50 mg fraction. This fraction was then purified by semi-preparative HPLC (YMC-Pack ODS-A column, 2.0 mL/min)

with 95% MeOH-THF to yield **6** (4.0 mg).

Purification process for **7**

The cells and culture medium extract (2.8 g) from 3 L culture of *S. cerevisiae* harboring *StaTC8* was separated using silica gel column chromatography with cyclohexane to give about 50 mg fraction. This fraction was then purified by semi-preparative HPLC (YMC-Pack ODS-A column, 2.0 mL/min) with 95% MeOH-THF to yield **7** (9.0 mg).

Purification process for **8** and **9**

The cells and culture medium extract (4.0 g) from 5 L culture of *S. cerevisiae* harboring *staTC4* was subjected to silica gel column chromatography with stepwise elution of cyclohexane and ethyl acetate (100:0 and 100:1, v/v) to afford fractions A and B. Fraction B (about 380 mg) was purified by semi-preparative HPLC (YMC-Pack ODS-A column, 2.0 mL/min) with 80% CH_3CN-H_2O to yield the mixture of **8** and **9**, which was further separated over a chiral HPLC column [Phenomenex i-Cellulose-5 (250 × 4.6 mm, 5 μm), 0.8 mL/min] with isocratic elution of 65% CH_3CN-H_2O to yield **8** (6.7 mg) and **9** (13.0 mg). In addition, we also isolated **8** and **9** from the *S. cerevisiae* transformants harboring *talTC1*, *wesTC*, *triTC*, or *mycTC*, respectively.

Structural characterization of compounds isolated in this study

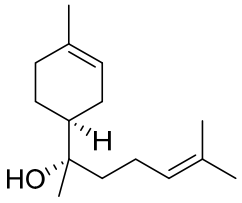

(–)-α-Bisabolol (**1**)

(–)-*α*-Bisabolol (**1**): colorless oil; $[\alpha]_D^{30}$ –43 (*c* 0.6, ethanol); EI-MS spectrum, see Fig. S2; NMR spectra, see Figs. S3−S4; ^{1}H NMR (400 MHz, $CDCl_3$) δ_H 5.37 (m, 1H), 5.13 (t, J = 7.1 Hz, 1H), 2.04 (m, 4H), 1.91 (m, 1H), 1.79 (m, 1H), 1.68 (s, 3H), 1.65 (s, 3H), 1.62 (s, 3H), 1.58 (m, 1H), 1.50 (td, J = 7.3, 3.2 Hz, 2H), 1.30 (m, 2H), 1.11 (s, 3H); ^{13}C NMR (100 MHz, $CDCl_3$) δ_C 134.1, 131.7, 124.6, 120.5, 74.4, 43.0, 40.1, 31.0, 26.9, 25.7, 23.3, 23.3, 23.2, 22.1, 17.7. The ^{13}C NMR data and the specific rotation value were in good agreement with those of (–)-*α*-bisabolol.[1]

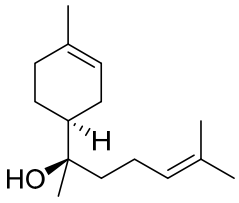

(–)-*epi*-α-Bisabolol (**2**)

(–)-*epi*-*α*-Bisabolol (**2**): colorless oil; $[\alpha]_D^{30}$ −94 (*c* 0.3, ethanol); EI-MS spectrum, see Fig. S2; NMR spectra, see Figs. S5−S6; ^{1}H NMR (400 MHz, $CDCl_3$) δ_H 5.40 (m, 1H), 5.13 (t, *J* = 7.1 Hz, 1H), 2.04 (m, 4H), 1.89 (m, 1H), 1.80 (m, 1H), 1.68 (s, 3H), 1.64 (s, 3H), 1.62 (s, 3H), 1.58 (m, 1H), 1.51 (t, *J* = 8.3 Hz, 2H), 1.30 (m, 2H), 1.13 (s, 3H); ^{13}C NMR (100 MHz, $CDCl_3$) δ_C 133.8, 131.7, 124.6, 120.8, 74.4, 43.4, 39.4, 31.1, 26.1, 25.7, 24.0, 24.0, 23.3, 22.3, 17.7. The ^{13}C NMR data and the specific rotation value were in good agreement with those of (–)-*epi*-*α*-bisabolol.[1]

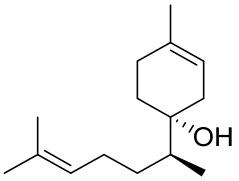

(–)-4-*epi*-β-Bisabolol (**3**)

(–)-4-*epi*-β-Bisabolol (**3**): colorless oil; $[\alpha]_D^{28}$ −42 (*c* 0.3, $CHCl_3$); EI-MS spectrum, see Fig. S2; NMR spectra, see Figs. S9−S10; ^{1}H NMR (400 MHz, $CDCl_3$) δ_H 5.30 (m, 1H), 5.10 (t, *J* = 7.4 Hz, 1H), 2.17 (m, 2H), 2.11 (m, 1H), 1.93 (m, 1H), 1.92 (m, 1H), 1.90 (m, 1H), 1.68 (br s, 6H), 1.61 (br s, 3H), 1.61 (m, 1H), 1.60 (m, 2H), 1.47 (m, 1H), 1.07 (m, 1H), 0.95 (d, *J* = 6.9 Hz, 3H); ^{13}C NMR (100 MHz, $CDCl_3$) δ_C 133.9, 131.4, 124.7, 118.4, 72.1, 41.8, 34.9, 30.9, 30.7, 27.0, 26.5, 25.7, 23.3, 17.7, 13.6. The ^{13}C NMR data and the specific rotation value were in good accordance with those of (–)-4-*epi*-β-bisabolol.[2, 3]

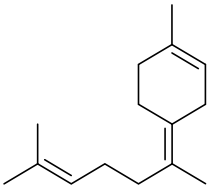

(*E*)-γ-Bisabolene (**4**)

(*E*)-γ-Bisabolene (**4**): colorless oil; EI-MS spectrum, see Fig. S2; NMR spectra, see Figs. S11−S12; ^{1}H NMR (400 MHz, $CDCl_3$) δ_H 5.37 (m, 1H), 5.14 (t, *J* = 6.4 Hz, 1H), 2.72 (br s, 2H), 2.32 (t, *J* = 6.3 Hz, 2H), 1.96−2.10 (m, 6H), 1.69 (s, 3H), 1.67 (s, 6H), 1.61 (s, 3H); ^{13}C NMR (100 MHz, $CDCl_3$) δ_C 134.2, 131.4, 128.3, 125.9, 124.5, 120.7, 34.2, 31.8, 29.7, 27.3, 26.5, 25.7, 23.4, 18.4, 17.6. The ^{13}C NMR data were in good accordance with those of (*E*)-γ-bisabolene.[4]

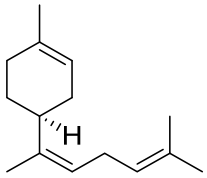

(+)-*Z*-α-Bisabolene (**5**)

(+)-*Z*-*α*-Bisabolene (**5**): colorless oil; $[\alpha]_D^{25}$ +13 (*c* 0.28, ethanol); EI-MS spectrum, see Fig. S2; NMR spectra, see Figs. S13−S14; ^{1}H NMR (400 MHz, $CDCl_3$) δ_H 5.42 (m, 1H), 5.10 (t, *J* = 7.0 Hz, 1H), 5.08 (t, *J* = 7.0 Hz, 1H), 2.70 (m, 2H), 2.65 (m, 1H), 2.02 (m, 2H), 1.99 (m, 1H), 1.83 (m, 1H), 1.69 (s, 3H), 1.66 (s, 3H), 1.62 (s, 6H), 1.58 (m, 2H); ^{13}C NMR (100 MHz, $CDCl_3$) δ_C 139.1, 133.8, 131.3, 123.6, 123.6, 121.0, 35.3, 30.6, 29.5, 27.5, 26.4, 25.7, 23.6, 19.3, 17.7. The ^{13}C NMR data and the specific rotation value were consistent with those of (+)-*Z*-*α*-bisabolene.[5]

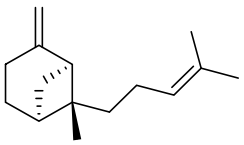

(–)-β-*trans*-Bergamotene (**6**)

(–)-β-*trans*-Bergamotene (**6**): colorless oil; $[\alpha]_D^{23}$ –22.4 (*c* 0.6, $CHCl_3$); EI-MS spectrum, see Fig. S2; NMR spectra, see Figs. S15−S16; ^{1}H NMR (400 MHz, $CDCl_3$) δ_H 5.16 (t, *J* = 7.0 Hz, 1H), 4.63 (br s, 1H), 4.56 (br s, 1H), 2.56 (m, 1H), 2.53 (t, *J* = 5.4 Hz, 1H), 2.28 (m, 1H), 2.25 (m, 1H), 2.06 (m, 1H), 1.95 (q, *J* = 7.9 Hz, 2H), 1.82 (m, 2H), 1.70 (s, 3H), 1.62 (s, 3H), 1.61 (m, 2H), 1.42 (br d, *J* = 9.9 Hz, 1H), 0.71 (s, 3H); ^{13}C NMR (100 MHz, $CDCl_3$) δ_C 152.2, 131.1, 125.1, 106.0, 50.2, 43.8, 38.7, 38.2, 27.1, 25.7, 23.8, 23.5, 23.5, 18.6, 17.6. The ^{13}C NMR data and the specific rotation value were in good agreement with those of (–)-β-*trans*-bergamotene.[6, 7]

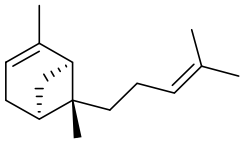

(–)-α-*trans*-Bergamotene (**7**)

(–)-α-*trans*-Bergamotene (**7**): colorless oil; $[\alpha]_D^{28}$ –35 (*c* 1.0, $CHCl_3$); EI-MS spectrum, see Fig. S2; NMR spectra, see Figs. S17−S22; NMR data, see Table S4; Based on NMR data analysis and comparison of the specific rotation value, **7** was established as the known compound (–)-α-*trans*-bergamotene.[8]

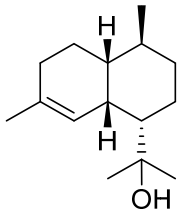

8

Compound **8**: white powder; $[\alpha]_D^{25}$ +8.0 (*c* 0.9, $CHCl_3$); EI-MS spectrum, see Fig. S2; HR-ESI-MS $[M + H - H_2O]^+$ *m/z* 205.1961 (calcd for $C_{15}H_{25}$, 205.1956), see Fig. S23; NMR spectra, see Figs. S24−S29; NMR data, see Table S5. Based on NMR data analysis, the relative configuration of **8** was determined as 1*R**,6*S**,7*S**,10*S**, which was identical to that of 4-amorphen-11-ol.[9]

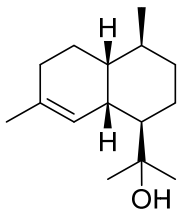

9

Compound **9**: colorless oil; $[\alpha]_D^{25}$ −16 (*c* 0.6, $CHCl_3$); EI-MS spectrum, see Fig. S2; HR-ESI-MS $[M + H - H_2O]^+$ *m/z* 205.1954 (calcd for $C_{15}H_{25}$, 205.1956), see Fig. S30; NMR spectra, see Figs. S31−S36; NMR data, see Table S6. Based on the NOESY spectrum, we determined that H-6, C-11, and C-14 located on the same side of the six-membered ring. With the aid of quantum chemical ^{13}C NMR calculation (Table S7), the relative configuration of **9** was determined as 1*R**,6*S**,7*R**,10*S**.

Quantum chemical ^{13}C NMR calculation of 9

The molecules of **9a** and **9b** were converted into SMILES codes before their initial 3D structures were generated with CORINA version 3.4. Conformer databases were generated in CONFLEX version 7.0 using the MMFF94s force-field, with an energy window for acceptable conformers (ewindow) of 5 kcal/mol above the ground state, a maximum number of conformations per molecule (maxconfs) of 100, and an RMSD cutoff (rmsd) of 0.5Å. Then each acceptable conformers was optimized with HF/6-31G(d) method in Gaussian09.[10] Further optimization at the wB97XD/6-31G(d) level determined the dihedral angles. From this, stable conformers (4 for **9a** and 15 for **9b**) were obtained (Fig. S37). The stable conformers were used for ^{13}C NMR calculations, which were performed with Gaussian09 (mPW1PW91/6-31+G(d,p)). The solvent was deuterated chloroform, and solvent effects were taken into account by the IEFPCM solvent model. TMS was

used as reference. The comparison was judged by R square (R^2) analysis, mean absolute error (MAE) and DP4+ probability (Table S7).[11]

Supplementary Tables

Table S1. Primers used in this study

Primer	5′-to-3′ sequence[a]	Usage
FusTC1-F	CTCACTATAGGGCCCATGGCTAGCAAATCTGTCAC	Construction of plasmid pESC-URA-*fusTC1*
FusTC1-R2	CAGAATGTTGGGTCGCTTCC	
FusTC1-F1	GGAAGCGACCCAACATTCTGCATGCAATACACAAGAGGAC	
FusTC1-R	TCCATGTCGACGCCCGGTGTTCGCTAGGCTATCAT	
StaTC1-F	CTCACTATAGGGCCCATGTCCCGTTTCTCTACTGCTATGGACGTGCCTAGACGGCTCTC	Construction of plasmid pESC-URA-*staTC1*
StaTC1-R	TCCATGTCGACGCCCTTACCACCCTAAGGTAGCGACCA	
StaTC1-N80A-F	CTTGCTTGCTTTCAATGTCGACGCCCAGAGACAGCCTTCGTCCATC	Construction of pESC-URA-*staTC1*-N80A mutant
StaTC1-N80A-R	GTCGACATTG.AAAGCAAGCAAG	
StaTC1-Q81A-F	GCTTGCTTTCAATGTCGACAACGCGAGACAGCCTTCGTCCATCC	Construction of pESC-URA-*staTC1*-Q81A mutant
StaTC1-Q81A-R	GTTGTCGACATTGAAAGCAAGCAAGTTCATCCAGAGC	
StaTC1-R82A-F	CTTTCAATGTCGACAACCAGGCACAGCCTTCGTCCATCCTCG	Construction of pESC-URA-*staTC1*-R82A mutant
StaTC1-R82A-R	CTGGTTGTCGACATTGAAAGCAAGC	
StaTC1-Q83A-F	TCAATGTCGACAACCAGAGAGCGCCTTCGTCCATCCTCGAAG	Construction of pESC-URA-*staTC1*-Q83A mutant
StaTC1-Q83A-R	TCTCTGGTTGTCGACATTGAAAGCAAGC	
StaTC1-P84A-F	ATGTCGACAACCAGAGACAGGCTTCGTCCATCCTCGAAGAC	Construction of pESC-URA-*staTC1*-P84A mutant
StaTC1-P84A-R	CTGTCTCTGGTTGTCGACATTGAAAGC	
StaTC1-S86A-F	ACAACCAGAGACAGCCTTCGGCCATCCTCGAAGACAAGCTTAAC	Construction of pESC-URA-*staTC1*-S86A mutant
StaTC1-S86A-R	CGAAGGCTGTCTCTGGTTGTCG	
StaTC1-E89A-F	GACAGCCTTCGTCCATCCTCGCCGACAAGCTTAACAAGCCGTG	Construction of pESC-URA-*staTC1*-E89A mutant
StaTC1-E89A-R	CGAGGATGGACGAAGGCTGTC	
StaTC1-D90A-F	GCCTTCGTCCATCCTCGAAGCCAAGCTTAACAAGCCGTGGAG	Construction of pESC-URA-*staTC1*-D90A mutant
StaTC1-D90A-R	CTTCGAGGATGGACGAAGGC	
StaTC1-D210A-F	ACAGATGCAGGACATGGCTGCCCAACCTGGCGACCGCATGCG	Construction of pESC-URA-*staTC1*-D210A mutant
StaTC1-D210A-R	CAGCCATGTCCTGCATCTGTATACTGG	
StaTC1-D214A-F	CATGGCTGACCAACCTGGCGCCCGCATGCGAGGCCGGAAAAC	Construction of pESC-URA-*staTC1*-D214A mutant
StaTC1-D214A-R	CGCCAGGTTGGTCAGCCATG	
MyrTC1-F	CTCACTATAGGGCCCATGTCTACCACAACCACAAC	Construction of plasmid pESC-URA-*myrTC1*

MyrTC1-R	TCCATGTCGACGCCCCTACCAGGCAAGTAGTGGCA	
MyrTC2-F	CTCACTATAGGGCCCATGGCCTCCAGGCTCCCATT	Construction of plasmid pESC-URA-*myrTC2*
MyrTC2-R	TCCATGTCGACGCCCTTATGACCTGGCGGTGAGTG	
MyrTC3-F	CTCACTATAGGGCCCATGACCTCAGTCGCCACATC	Construction of plasmid pESC-URA-*myrTC3*
MyrTC3-R	TCCATGTCGACGCCCTCATAGAAGCGCCACGCTCG	
MyrTC4-F	CTCACTATAGGGCCCATGGAAGGATACACTTCTTACGC	Construction of plasmid pESC-URA-*myrTC4*
MyrTC4-R	TCCATGTCGACGCCCTCACATCGATGTTGGTCCTC	
StaTC2-F	CTCACTATAGGGCCCATGTCACAATTACATGACACCGC	Construction of plasmid pESC-URA-*staTC2*
StaTC2-R	TCCATGTCGACGCCCTCATGCTTTCCAGAGCGGCA	
StaTC3-F	CTCACTATAGGGCCCATGTCGGTGAAGGGCACGTC	Construction of plasmid pESC-URA-*staTC3*
StaTC3-R	TCCATGTCGACGCCCTTAGTGCCTGCTCAATAGAGGGAG	
StaTC4-F	CTCACTATAGGGCCCATGACGCCCACACACAGTTC	Construction of plasmid pESC-URA-*staTC4*
StaTC4-R	TCCATGTCGACGCCCCTATTGGATTGGAGAATTCG	
StaTC5-F	CTCACTATAGGGCCCATGACTTATACGCAGCGGAG	Construction of plasmid pESC-URA-*staTC5*
StaTC5-R	TCCATGTCGACGCCCTTAAAGCCCTTGCAAGAGCG	
StaTC6-F	CTCACTATAGGGCCCATGGATATGGACATGATCCG	Construction of plasmid pESC-URA-*staTC6*
StaTC6-R	TCCATGTCGACGCCCTTACCAGGAGCTCGCTTGGT	
StaTC7-F	CTCACTATAGGGCCCATGGCGGAAACTGTGAGAAT	
StaTC7-R1	ATGCCGACTGGCGGTTCCGA	Construction of plasmid pESC-URA-*staTC7*
StaTC7-F1	TCGGAACCGCCAGTCGGCATACATCATGTTCGACTTCGTC	
StaTC7-R	TCCATGTCGACGCCCTTATCGGACCGTCAAGTTCT	
StaTC8-F	CTCACTATAGGGCCCATGACTGCCTCAACACCCTC	Construction of plasmid pESC-URA-*staTC8*
StaTC8-R	TCCATGTCGACGCCCCTATGACAGGTGGCGAGCCA	
BisTC1-F	CTCACTATAGGGCCCATGACCCGCCTCATCCCGGA	Construction of plasmid pESC-URA-*bisTC1*
BisTC1-R	TCCATGTCGACGCCCTCATAAGTCCAAAACTGGCCTC	
BisTC2-F	CTCACTATAGGGCCCATGACAAACACGGTCTTTCA	
BisTC2-R1	AAACAACGCTTGCTCCATGTAATAGTTGAACGAGACATAT	Construction of plasmid pESC-URA-*bisTC2*
BisTC2-F1	ACATGGAGCAAGCGTTGTTT	
BisTC2-R	TCCATGTCGACGCCCTTAACCTGCGCTGGCCAATG	
MycTC-F	CTCACTATAGGGCCCATGGCCAGCCCACTGCAGTC	Construction of plasmid pESC-URA-*mycTC*
MycTC-R	TCCATGTCGACGCCCCTAGTTAAGAAGAGCGTGGACCAC	
TalTC1-F	CTCACTATAGGGCCCATGCATGGACAACCGAAAAACGTTGACGCGTCTCTAAAAATGGGCTCC	
TalTC1-F1	CGTCTCTAAAAATGGGCTCCGAGCATCGCTTCCGAAAGCAATCGGCCTCTCTATTCTC	Construction of plasmid pESC-URA-*talTC1*
TalTC1-R	TCCATGTCGACGCCCTCAATACCCGATTAATGTGG	

TalTC2-F	CTCACTATAGGGCCCATGGAGGCAATTGGCTCAACTCCCACTCTGGCGGCGTCTGGCC	Construction of plasmid pESC-URA-*talTC2*
TalTC2-F1	CAAAGACCATGGGAAAATCACCCTTTACCGAGCATAAAGGCGCCTTGCTACACAT	
TalTC2-F2	CACTCTGGCGGCGTCTGGCCACACAGAAAAATCAAAGACCATGGGAAAATCA	
TalTC2-R	TCCATGTCGACGCCCTCAGATCGCGAGTGGTAGCA	
ColTC-F	CTCACTATAGGGCCCATGTCTGCTCAAGAAGATAG	Construction of plasmid pESC-URA-*colTC*
ColTC-R	TCCATGTCGACGCCCTTAAGCAACGAACAATGGCAAAA	
WesTC-F	CTCACTATAGGGCCCATGGCTTCTAGATCTGCTAA	Construction of plasmid pESC-URA-*wesTC*
WesTC-R	TCCATGTCGACGCCCTTAGAAAGTAGCGAACATTGGCA	
PenTC-F	CTCACTATAGGGCCCATGGCTATTAAGTCTTTGTG	Construction of plasmid pESC-URA-*penTC*
PenTC-R	TCCATGTCGACGCCCTTAACCAACGTCACCAGACAATT	
TriTC-F	CTCACTATAGGGCCCATGGGTAACGATGTTTTGTT	Construction of plasmid pESC-URA-*triTC*
TriTC-R	TCCATGTCGACGCCCTTACTTAGCCAAAGCTGGCAACA	
Gal-1-F	CATTTTCGGTTTGTATTACTTC	Universal primer for plasmid sequencing
Gal-1-R	GACCTAGACTTCAGGTTGTC	

[a] Modified codons for site-directed mutagenesis are underlined.

Table S2. Detailed information of 22 UbiA-type TCs used in this study

Protein	Accession No.	Fungal species	Product	Source
FusTC1	OM891474	*Fusarium* sp. JNU-XJ070152-01	**1**, **2**	Our lab
StaTC1	OM891475	*Stachybotrys* sp. PYH05-7	**1**	Our lab
StaTC2	OM891476	*Stachybotrys* sp. PYH05-7	**3**	Our lab
StaTC3	OM891477	*Stachybotrys* sp. PYH05-7	-	Our lab
StaTC4	OM891478	*Stachybotrys* sp. PYH05-7	**8**, **9**	Our lab
StaTC5	OM891479	*Stachybotrys* sp. PYH05-7	**6**	Our lab
StaTC6	OM891480	*Stachybotrys* sp. PYH05-7	**2**	Our lab
StaTC7	OM891481	*Stachybotrys* sp. PYH05-7	-	Our lab
StaTC8	OM891482	*Stachybotrys* sp. PYH05-7	**7**	Our lab
BisTC1	OM891483	*Biscogniauxia* sp. 71-10-1-1	-	Our lab
BisTC2	OM891484	*Biscogniauxia* sp. 71-10-1-1	-	Our lab
TalTC1	OM891485	*Talaromyces* sp. JNU18266-01	**8**, **9**	Our lab
TalTC2	OM891486	*Talaromyces* sp. JNU18266-01	**4**	Our lab
MycTC	OM891487	*Mycoleptodiscus* sp. JNU2018AT0063Y	**8**, **9**	Our lab
MyrTC1	OM891488	*Myrothecium* sp. ZL0801-19	-	Our lab
MyrTC2	OM891489	*Myrothecium* sp. ZL0801-19	-	Our lab
MyrTC3	OM891490	*Myrothecium* sp. ZL0801-19	**2**	Our lab
MyrTC4	OM891491	*Myrothecium* sp. ZL0801-19	**5**	Our lab
ColTC	EQB53108.1	*Colletotrichum gloeosporioides* Cg-14	-	NCBI
TriTC	PTB76894.1	*Trichoderma longibrachiatum* ATCC 18648	**8**, **9**	NCBI
WesTC	XP_033655798.1	*Westerdykella ornata*	**8**, **9**	NCBI
PenTC	KAF4766328.1	*Penicillium* sp. str. #12	-	NCBI

Table S3. Sequence identities (%) of 22 UbiA-type TCs used in this study

Seq->	FusTC1	StaTC1	StaTC2	StaTC4	StaTC5	StaTC6	StaTC8	TalTC1	TalTC2	MycTC	MyrTC3	MyrTC4	TriTC	WesTC
FusTC1	**ID**	**36.6**	**29.5**	**31.8**	**31.5**	**28.6**	**30.3**	**30.6**	**31.3**	**30.9**	**32.4**	**29.4**	**29.6**	**28.7**
StaTC1		**ID**	**39.3**	**34.8**	**34.3**	**32.9**	**33.4**	**37.0**	**36.2**	**33.3**	**36.7**	**33.0**	**32.9**	**29.8**
StaTC2			**ID**	**32.7**	**30.2**	**30.5**	**32.0**	**33.5**	**34.3**	**37.0**	**30.0**	**30.8**	**37.8**	**33.5**
StaTC4				**ID**	**32.5**	**29.7**	**31.9**	**36.3**	**28.1**	**35.3**	**34.8**	**32.3**	**43.5**	**31.7**
StaTC5					**ID**	**29.4**	**40.6**	**30.4**	**32.6**	**33.3**	**44.7**	**30.9**	**35.3**	**31.4**
StaTC6						**ID**	**27.8**	**31.1**	**30.2**	**31.3**	**28.4**	**28.7**	**28.9**	**35.7**
StaTC8							**ID**	**29.3**	**33.9**	**32.8**	**38.2**	**33.8**	**31.5**	**29.6**
TalTC1								**ID**	**31.0**	**42.0**	**31.3**	**32.5**	**40.8**	**30.5**
TalTC2									**ID**	**34.4**	**34.9**	**40.1**	**38.2**	**32.3**
MycTC										**ID**	**31.9**	**33.2**	**43.6**	**31.4**
MyrTC3											**ID**	**32.3**	**34.2**	**32.1**
MyrTC4												**ID**	**36.2**	**31.6**
TriTC													**ID**	**33.9**
WesTC														**ID**

The red colored number indicates the identity between StaTC6 and MyrTC3, and the bule colored numbers indicate the identities among StaTC4, TalTC1, MycTC, TriTC and WesTC.

Table S4. NMR data of compound 7 in $CDCl_3$

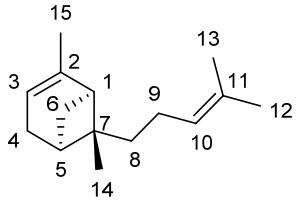

7

No.	δ_C[a], type	δ_H (J in Hz)[b, d]	^1H–^1H COSY[b]	HMBC[b]	NOESY[c]
1	45.4, CH	2.00	6a, 6b		
2	144.5, C				
3	116.4, CH	5.21	4a, 4b, 15	1, 4, 5, 15	14
4	31.2, CH_2	a: 2.25	3, 4b, 5	2, 3, 7	
		b: 2.15	3, 4a, 5	2, 3, 6	
5	38.9, CH	2.14	4a, 4b, 6a, 6b	3, 4, 6	
6	31.6, CH_2	a: 2.31	1, 5, 6b	5	8
		b: 1.16, br d (8.5)	1, 5, 6a	2, 4, 7	
7	41.1, C				
8	38.6, CH_2	1.61	9	1, 5, 7, 9, 10, 14	6a
9	23.8, CH_2	1.99	8, 10	8	
10	125.3, CH	5.17, br t (7.1)	9, 12, 13	9, 12, 13	12
11	131.0, C				
12	25.7, CH_3	1.70, br s	10	10, 11, 13	10
13	17.6, CH_3	1.63, br s	10	10, 11, 12	
14	17.4, CH_3	0.83, s		1, 5, 7, 8	3
15	23.0, CH_3	1.66, d (1.2)	3	1, 2, 3	

[a] The data were measured at 100 MHz.

[b] The data were measured at 400 MHz.

[c] The data were measured at 600 MHz.

[d] The indiscernible signals from overlap or the complex multiplicity are reported without designating multiplicity.

Table S5. NMR data of compound 8 in $CDCl_3$

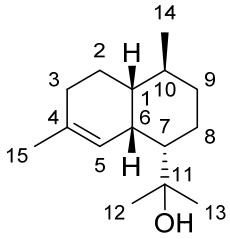

8

No.	δ_C[a], type	δ_H (J in Hz)[b, d]	^1H–^1H COSY[c]	HMBC[b]	NOESY[b]
1	42.5, CH	1.19	2a, 2b, 6, 10	2, 3, 5, 6, 9, 14	9b, 14
2	25.9, CH_2	a: 1.92	1, 2b, 3a, 3b	1, 3, 4, 6, 10	14
		b: 1.55	1, 2a, 3a, 3b	1, 3, 4, 6, 10	6
3	26.4, CH_2	a: 1.89	2a, 2b, 3b	1, 2, 4, 5	
		b: 1.78	2a, 2b, 3a	1, 2, 4, 5	
4	134.6, C				
5	122.1, CH	5.66	6, 15	1, 3, 6, 7, 15	12, 13
6	38.4, CH	2.65	1, 5, 7, 15	5, 8	2b, 12
7	51.4, CH	1.32, ddd (12.5, 3.7, 2.1)	6, 8a, 8b	1, 5, 6, 8, 9, 12	9b
8	22.9, CH_2	a: 1.61	7, 8b, 9a, 9b	6, 7, 9, 10, 11	
		b: 1.27	7, 8a, 9a, 9b	6, 9	
9	36.0, CH_2	a: 1.73, dq (12.5, 3.4)	8a, 8b, 9b, 10	1, 7, 8, 10, 14	14
		b: 0.97, qd (12.5, 3.4)	8a, 8b, 9a, 10	1, 7, 8, 10	1, 7
10	27.8, CH	1.48	1, 9a, 9b, 14	1, 2, 8, 9, 14	
11	73.1, C				
12	28.0, CH_3	1.29, s		7, 11, 13	5, 6
13	30.6, CH_3	1.26, s		7, 11, 12	5
14	19.8, CH_3	0.87, d (6.6)	10	1, 9, 10	1, 2a, 9a
15	23.9, CH_3	1.62	5, 6	3, 4, 5	

[a] The data were measured at 100 MHz.

[b] The data were measured at 600 MHz.

[c] The data were measured at 400 MHz.

[d] The indiscernible signals from overlap or the complex multiplicity are reported without designating multiplicity.

Table S6. NMR data of compound 9 in $CDCl_3$

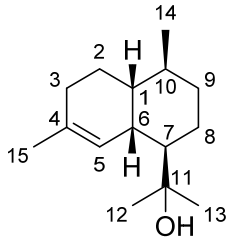

9

NO.	δ_C[a], type	δ_H (J in Hz)[b, d]	^1H–^1H COSY[c]	HMBC[b]	NOESY[b]
1	39.9, CH	1.51	2a, 2b, 6, 10	2, 3, 5, 6, 7, 9, 10, 14	
2	25.3, CH_2	a: 1.92	1, 2b, 3a, 3b	1, 3, 4, 6	
		b: 1.44	1, 2a, 3a, 3b	1, 3, 4, 6	
3	29.3, CH_2	a: 1.94	2a, 2b, 3b	1, 2, 4, 5	
		b: 1.91	2a, 2b, 3a	1, 2, 4, 5	
4	135.6, C				
5	126.3, CH	5.51	6, 15	1, 3, 6, 7, 15	7, 12, 13
6	34.5, CH	2.32	1, 5, 7, 15	1, 2, 4, 5, 7, 8, 10, 11	8b, 12, 13, 14
7	51.0, CH	1.45	6, 8a, 8b	1, 5, 6, 8, 9, 11, 12, 13	5
8	23.3, CH_2	a: 1.50	7, 8b, 9a, 9b	6, 7, 9, 10, 11	
		b: 1.34	7, 8a, 9a, 9b	6, 7, 9, 10, 11	6
9	29.0, CH_2	a: 1.59	8a, 8b, 9b, 10	1, 7, 8, 10, 14	14
		b: 1.31	8a, 8b, 9a, 10	1, 7, 8, 10, 14	
10	31.5, CH	1.62	1, 9a, 9b, 14	1, 2, 6, 8, 9, 14	
11	74.4, C				
12	26.2, CH_3	1.23, s		7, 11, 13	5, 6
13	29.9, CH_3	1.19, s		7, 11, 12	5, 6
14	19.7, CH_3	0.97, d (6.9)	10	1, 9, 10	6, 9a
15	23.7, CH_3	1.65	5, 6	3, 4, 5	

[a] The data were measured at 100 MHz.

[b] The data were measured at 600 MHz.

[c] The data were measured at 400 MHz.

[d] The indiscernible signals from overlap or the complex multiplicity are reported without designating multiplicity.

Table S7. R square (R^2) of the linear correlations, mean absolute error (MAE) values, and DP4+ probability analysis of 9a and 9b

NO.	**9** (Experimental)	**9a** (Calculated)	**AE**	**9b** (Calculated)	**AE**
C-1	39.9	42.19	2.29	39.30	0.60
C-2	25.3	29.17	3.87	26.02	0.72
C-3	29.3	30.94	1.64	27.94	1.36
C-4	135.6	133.34	2.26	135.77	0.17
C-5	126.3	125.85	0.45	126.79	0.49
C-6	34.5	36.71	2.21	37.19	2.69
C-7	51.0	52.94	1.94	50.65	0.35
C-8	23.3	23.80	0.50	24.35	1.05
C-9	29.0	33.30	4.30	30.29	1.29
C-10	31.5	33.62	2.12	31.03	0.47
C-11	74.4	73.19	1.21	72.62	1.78
C-12	26.2	20.46	5.74	27.40	1.20
C-13	29.9	29.96	0.06	27.63	2.27
C-14	19.7	11.09	8.61	19.12	0.58
C-15	23.7	22.99	0.71	23.50	0.20
MAE		2.53		1.01	
R^2		0.9911		0.9988	
DP4+		0.00%		100.00%	

AE: absolute error.

Supplementary Figures

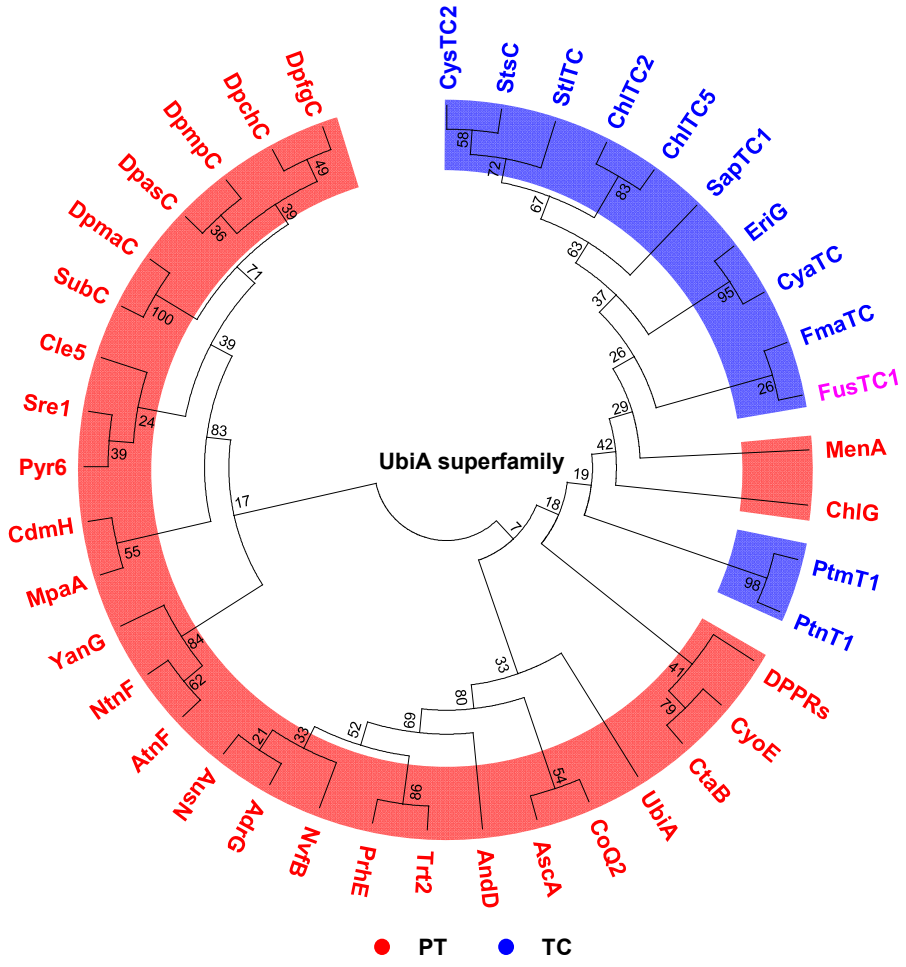

Fig. S1. Phylogenetic analysis of UbiA superfamily proteins from bacteria and fungi.

The protein sequences were aligned using ClustalW, and the tree was constructed by MEGA 7.0 software using the maximum likelihood method.

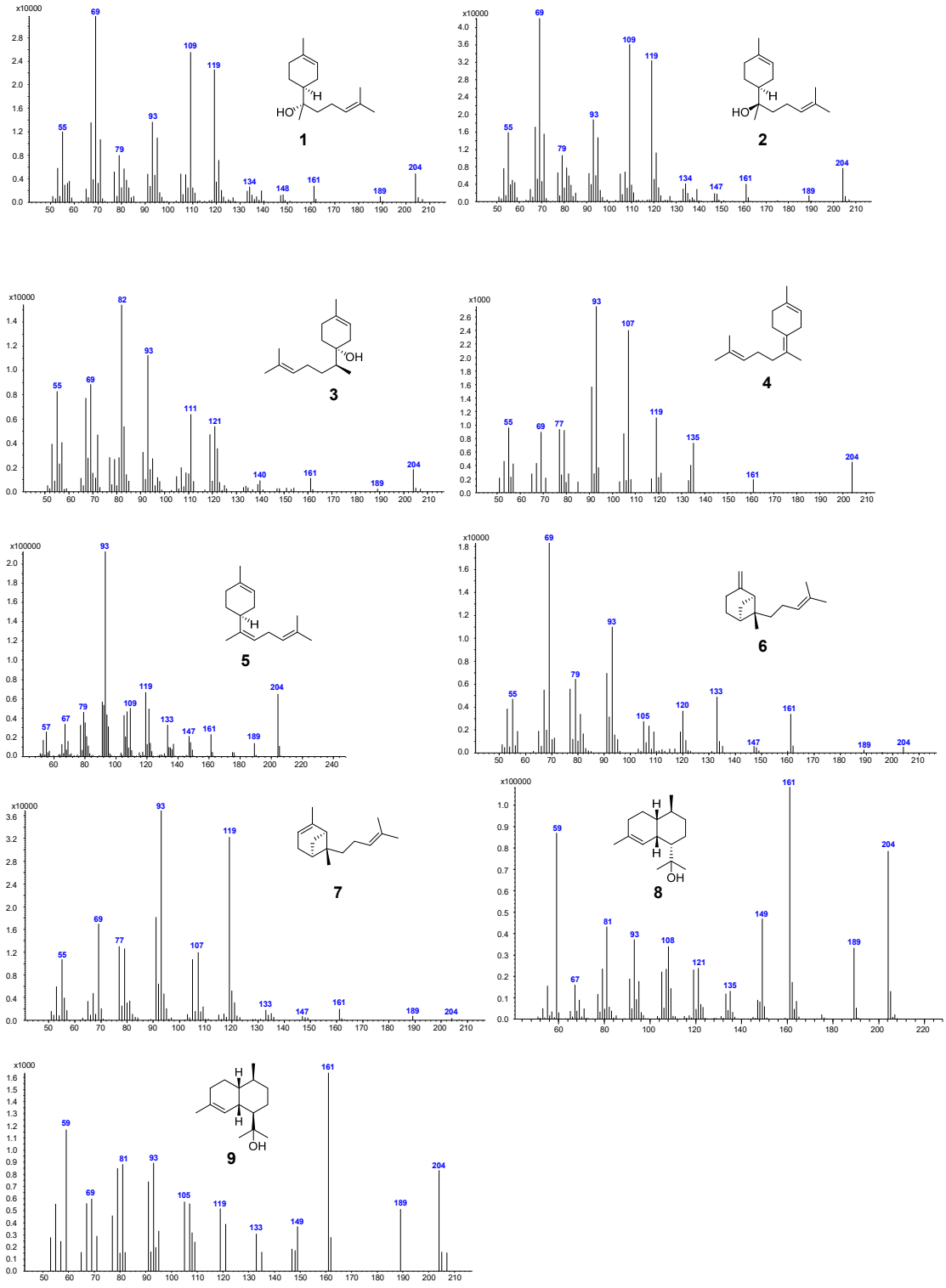

Fig. S2. Electron impact mass spectra of sesquiterpenes isolated in this study

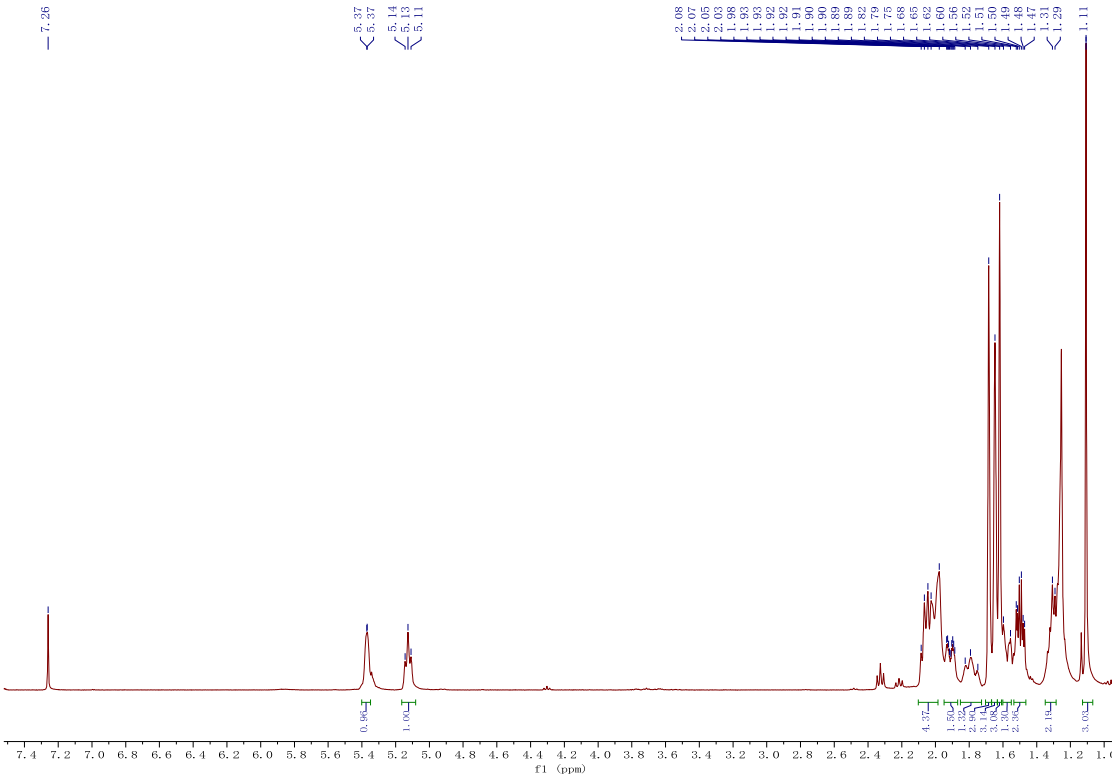

Fig. S3. ^{1}H NMR spectrum of 1 in $CDCl_3$ at 400 MHz

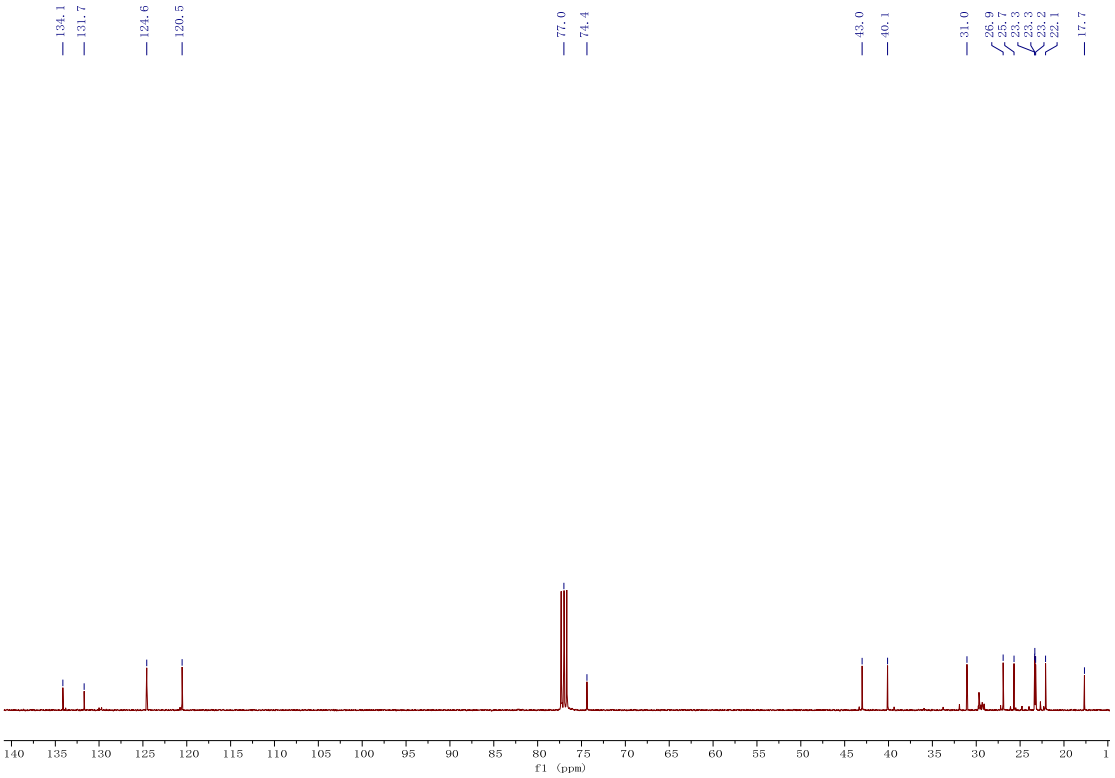

Fig. S4. ^{13}C NMR spectrum of 1 in $CDCl_3$ at 100 MHz

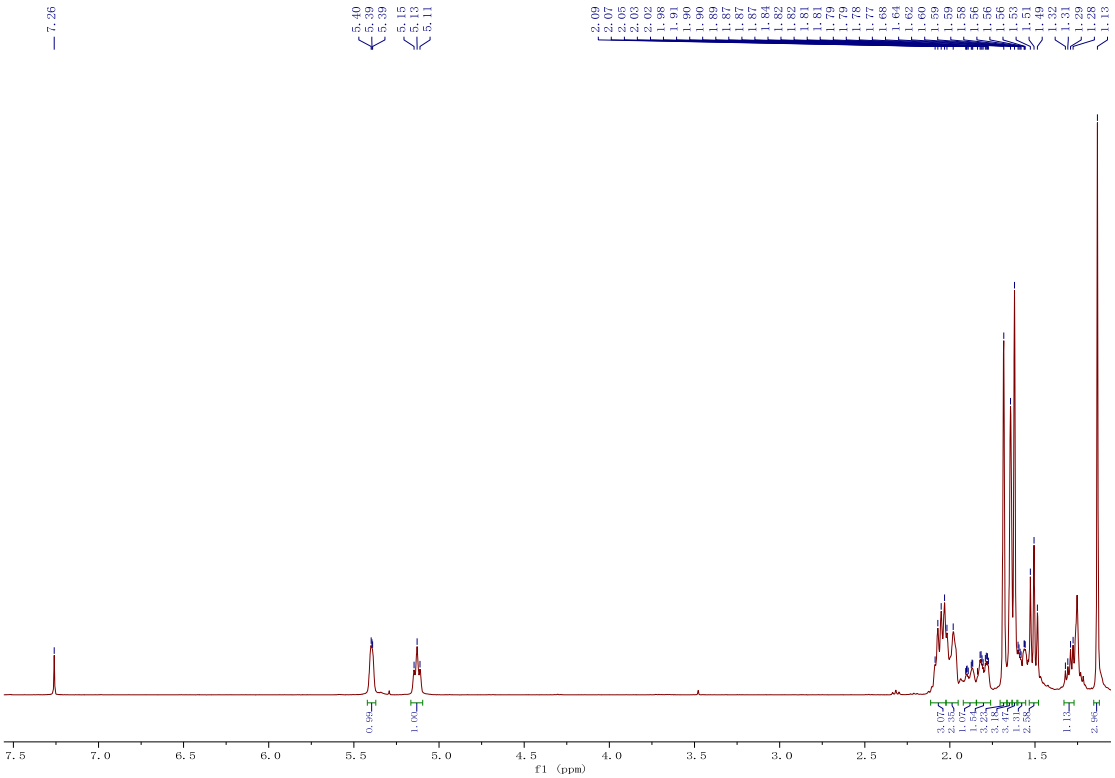

Fig. S5. ^{1}H NMR spectrum of 2 in $CDCl_3$ at 400 MHz

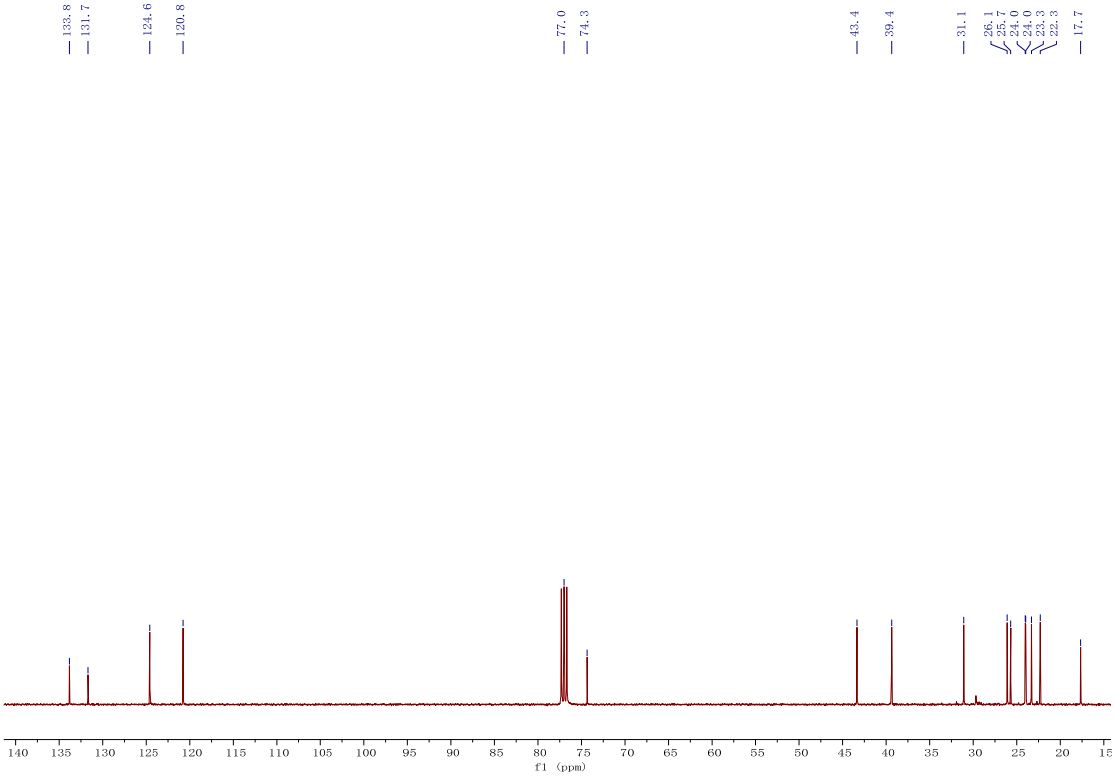

Fig. S6. ^{13}C NMR spectrum of 2 in $CDCl_3$ at 100 MHz

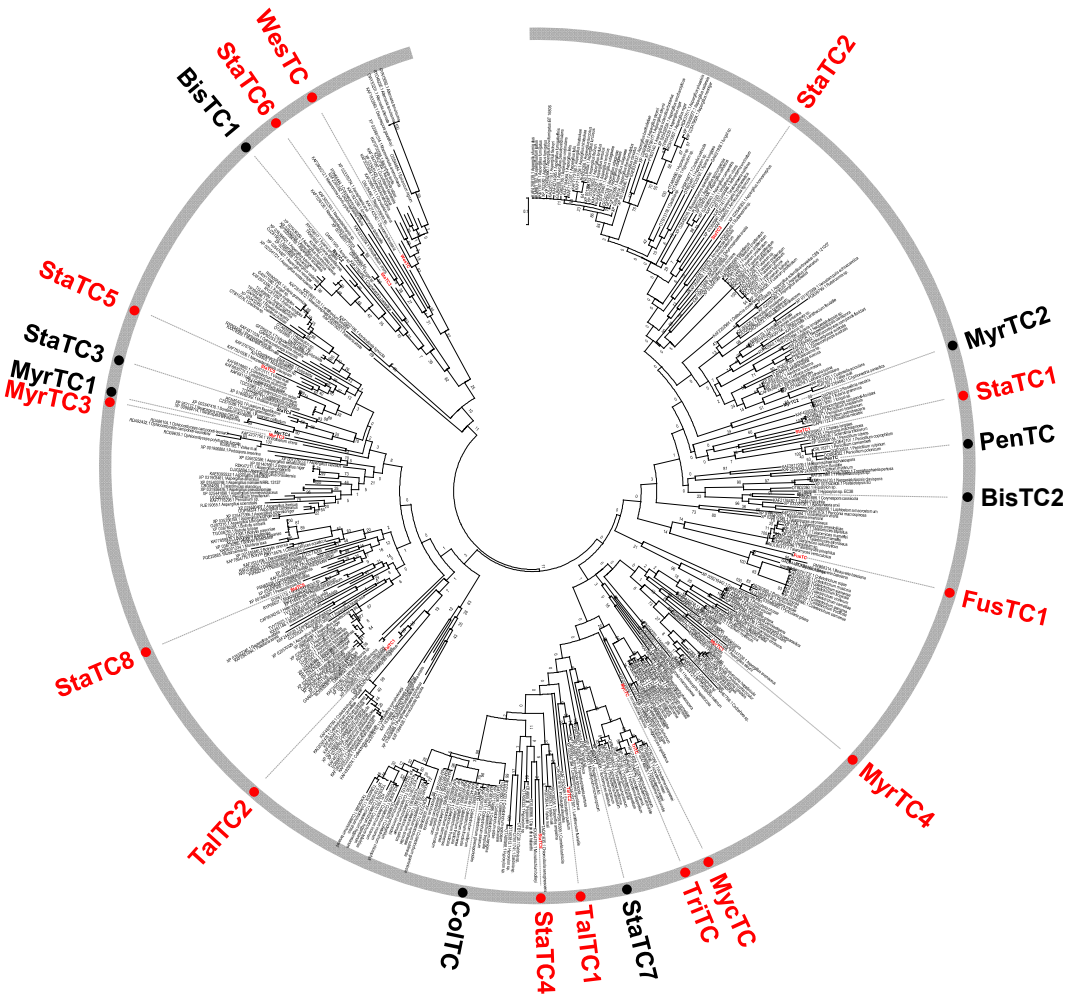

Fig. S7. Phylogenetic analysis of 485 UbiA-type TCs

The full-length protein sequences were aligned using ClustalW. A rooted maximum likelihood tree was generated using poisson model by MEGA 7.0 software with bootstrapping for 500 replicates. Selected cyclases for functional analysis are marked with dots, in which red coloured enzymes can produce sesquiterpenes in the engineered *S. cerevisiae*, and black coloured enzymes cannot yield products in the heterologous host.

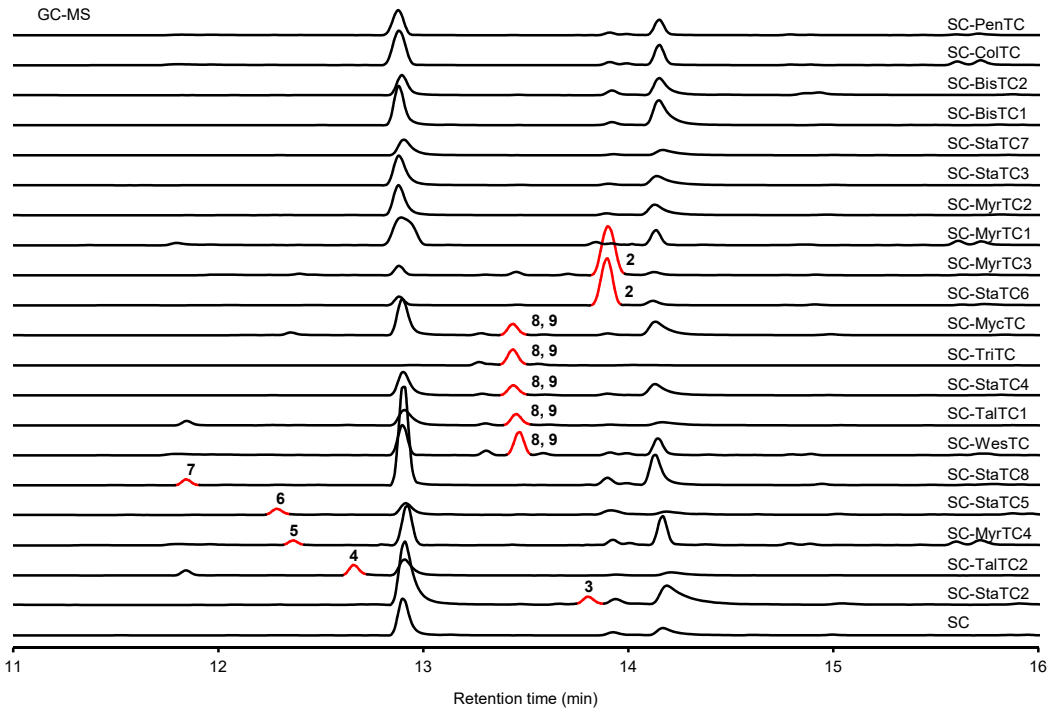

Fig. S8. GC-MS analysis of crude extracts of the *S. cerevisiae* transformants harboring the selected UbiA-type TCs

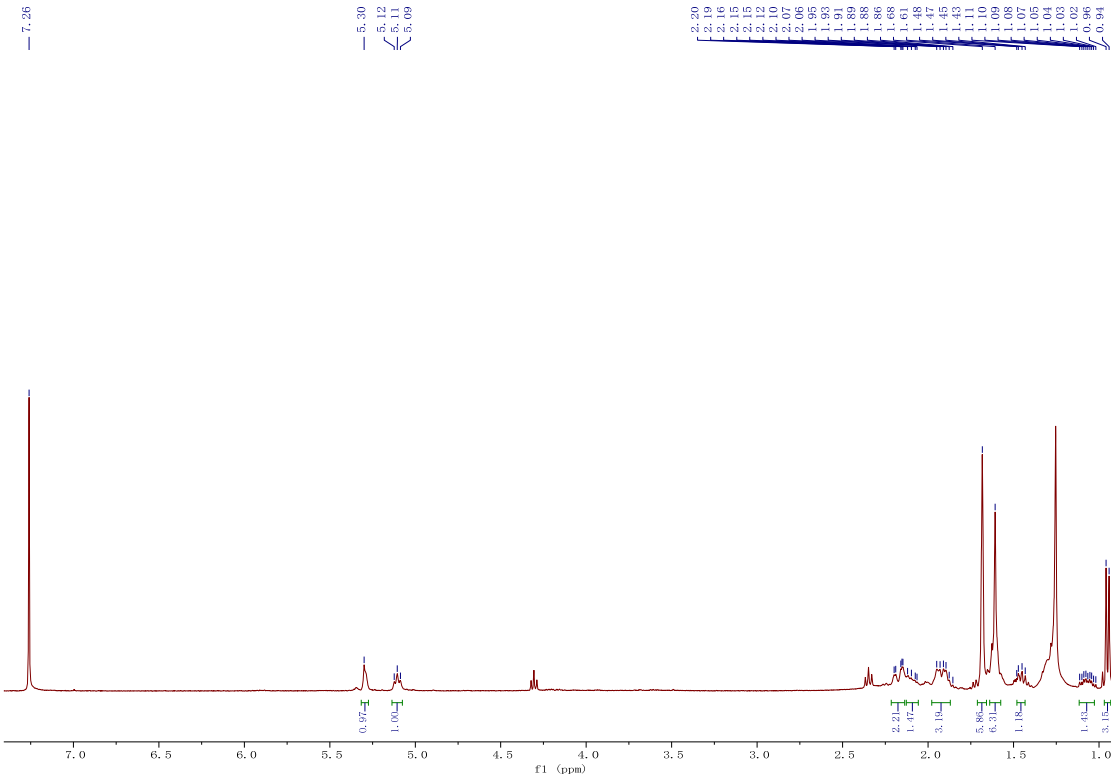

Fig. S9. ^{1}H NMR spectrum of 3 in $CDCl_3$ at 400 MHz

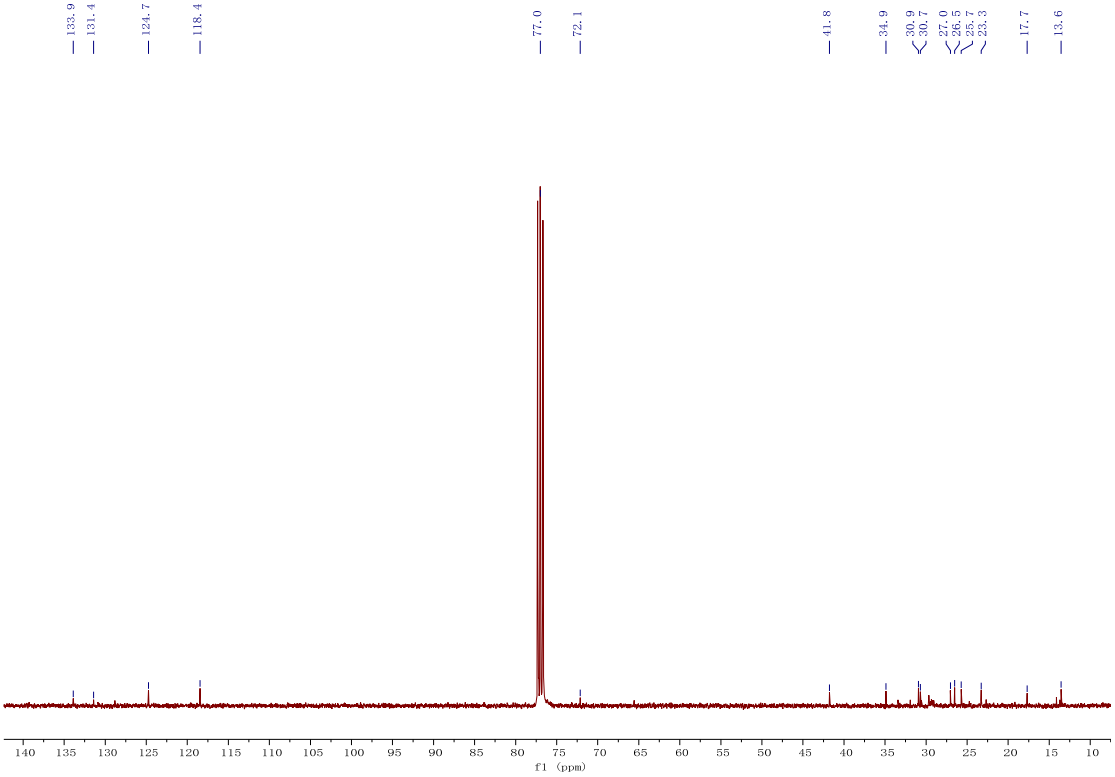

Fig. S10. ^{13}C NMR spectrum of 3 in $CDCl_3$ at 100 MHz

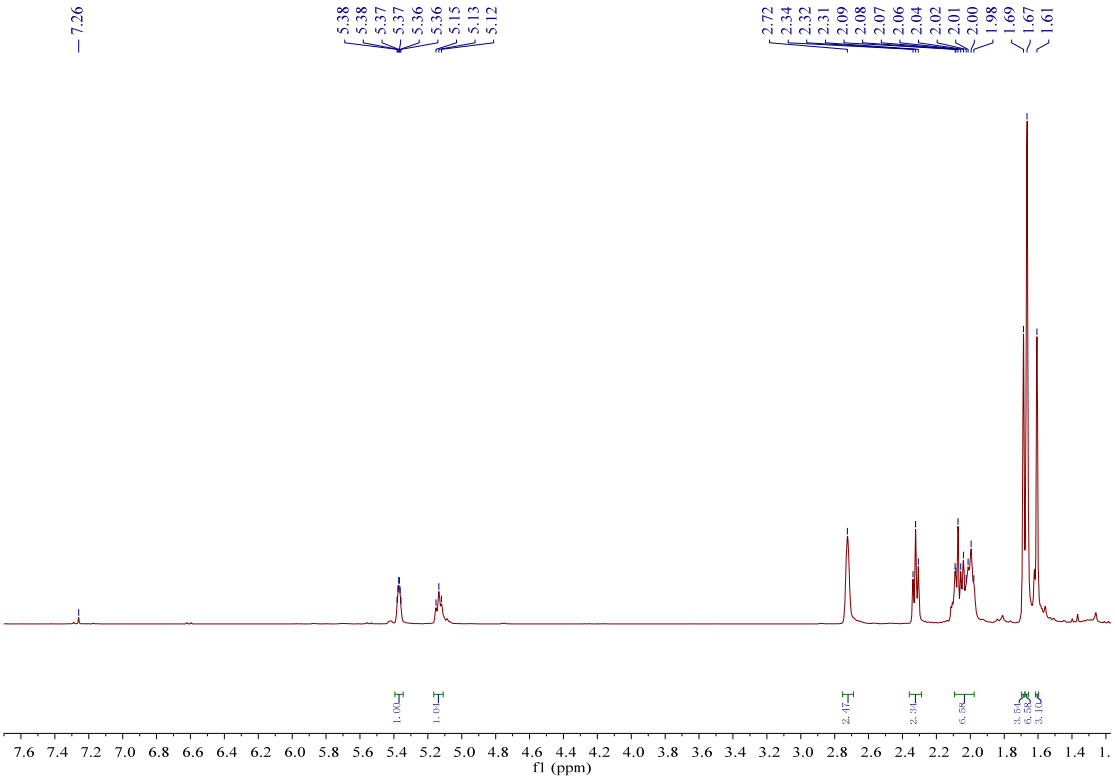

Fig. S11. ^{1}H NMR spectrum of 4 in $CDCl_3$ at 400 MHz

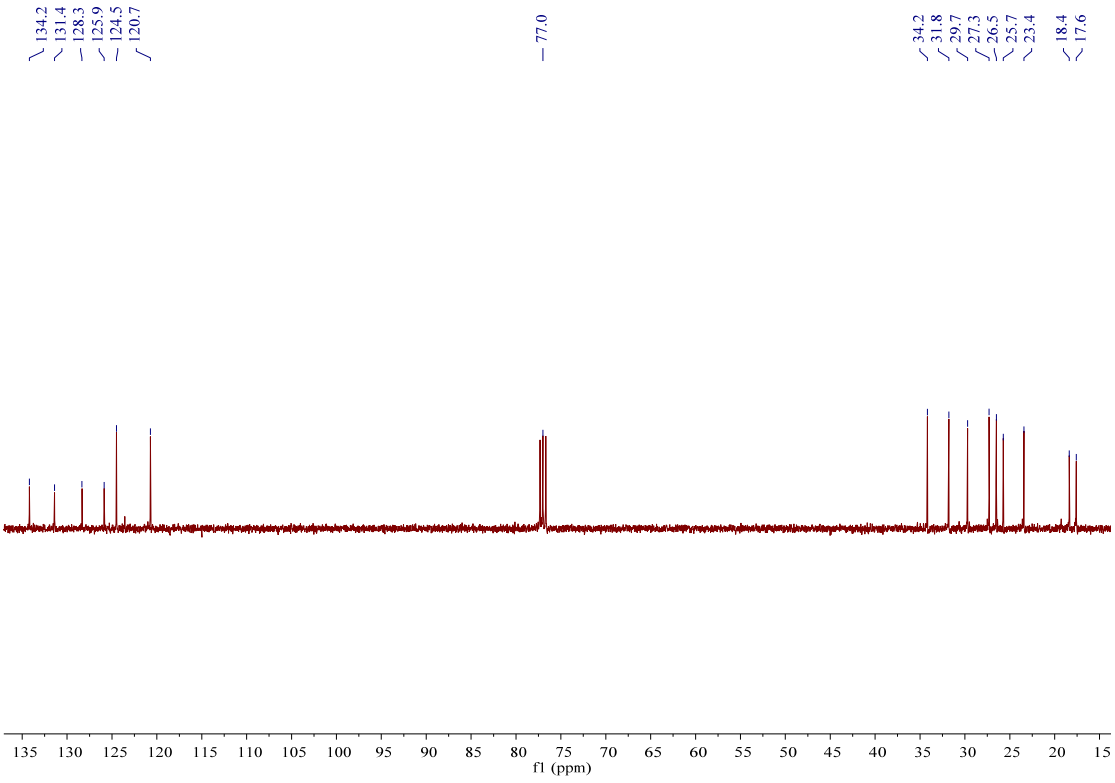

Fig. S12. ^{13}C NMR spectrum of 4 in $CDCl_3$ at 100 MHz

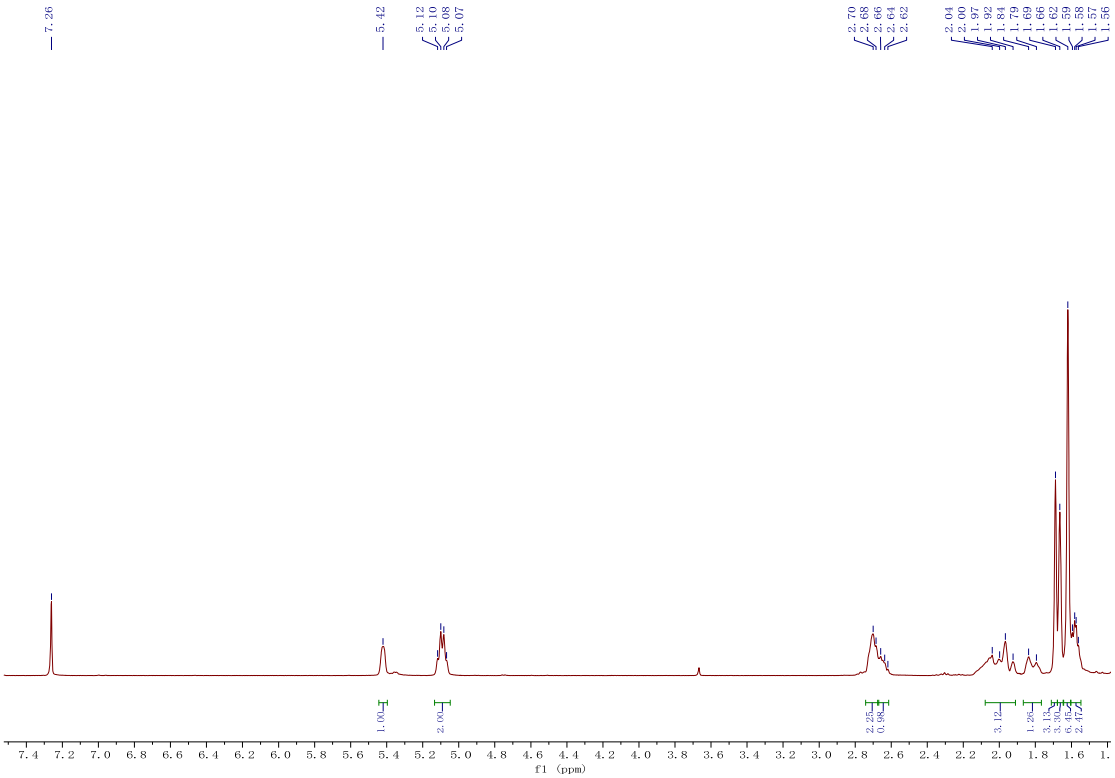

Fig. S13. ^{1}H NMR spectrum of 5 in $CDCl_3$ at 400 MHz

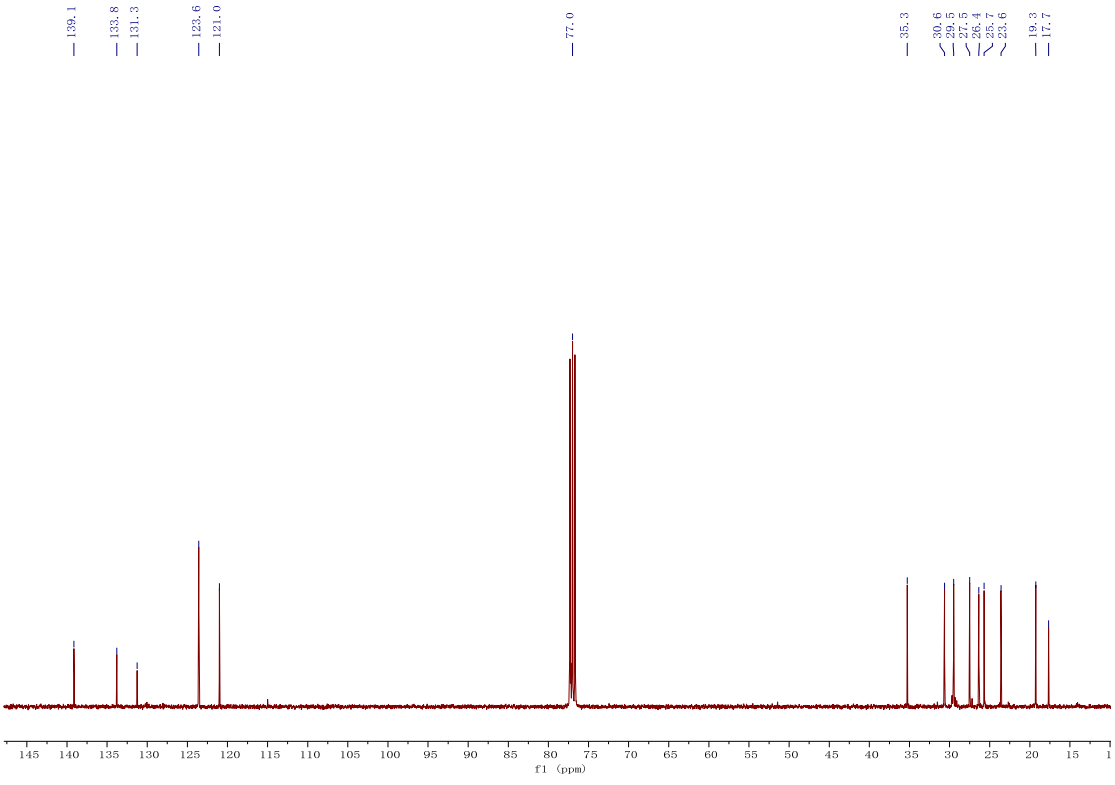

Fig. S14. ^{13}C NMR spectrum of 5 in $CDCl_3$ at 100 MHz

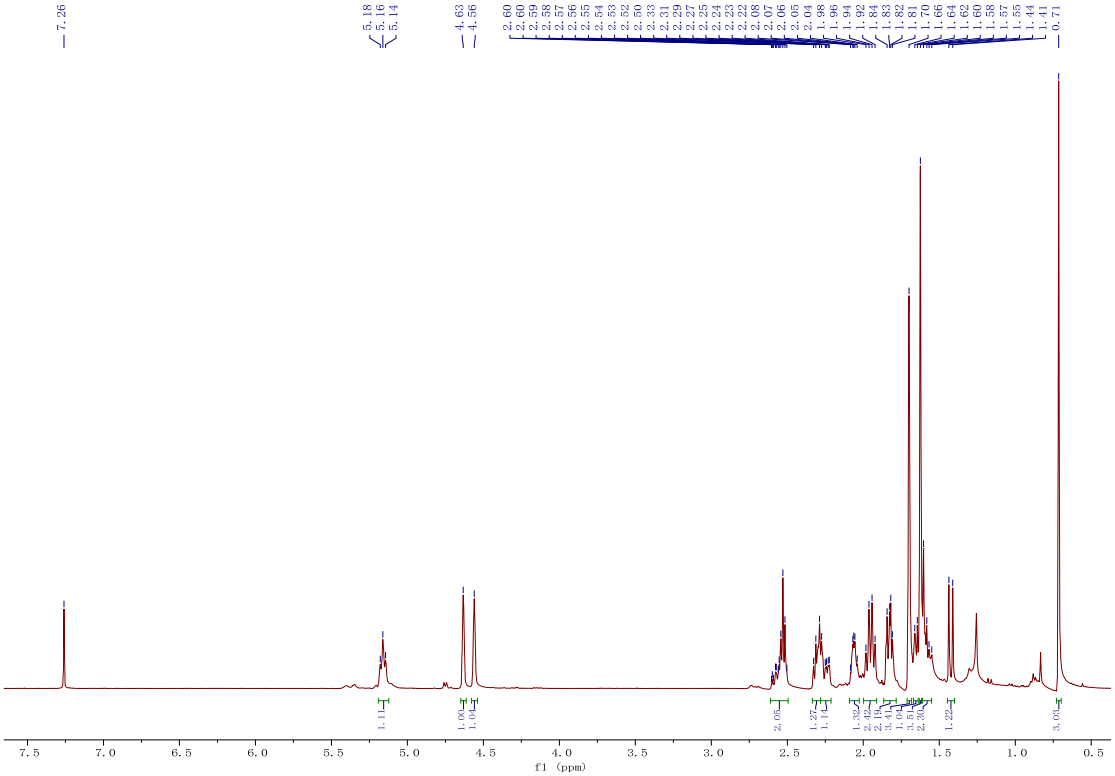

Fig. S15. ^{1}H NMR spectrum of 6 in $CDCl_3$ at 400 MHz

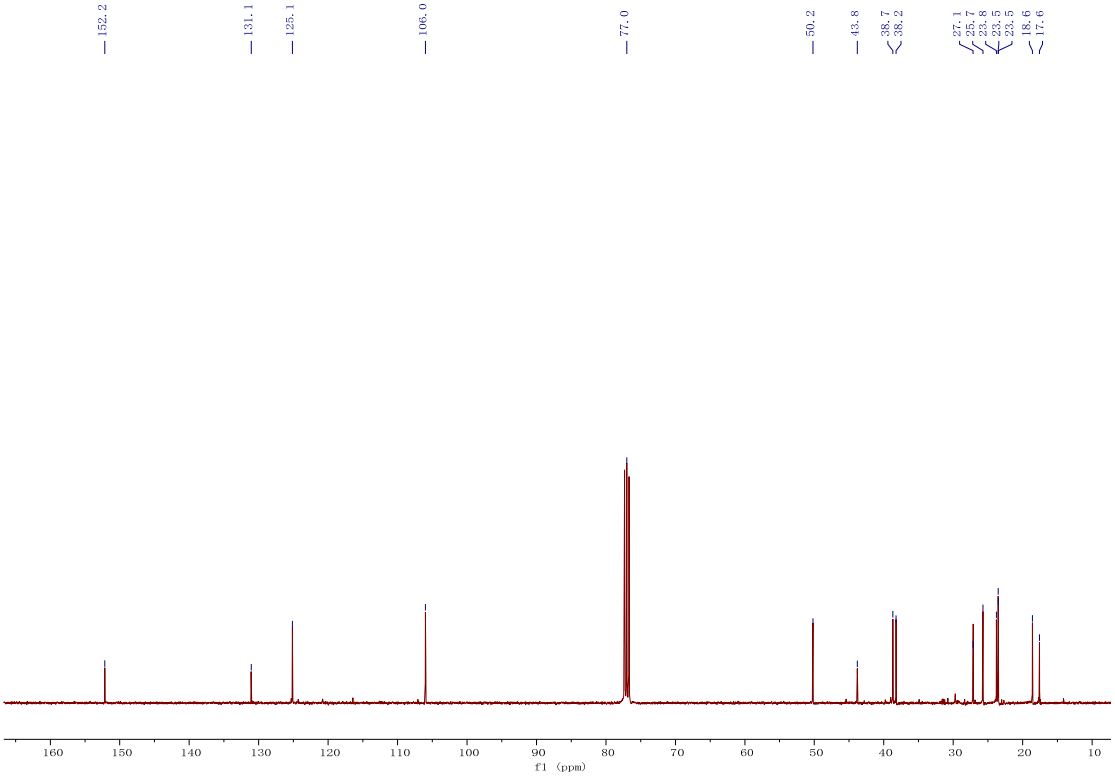

Fig. S16. ^{13}C NMR spectrum of 6 in $CDCl_3$ at 100 MHz

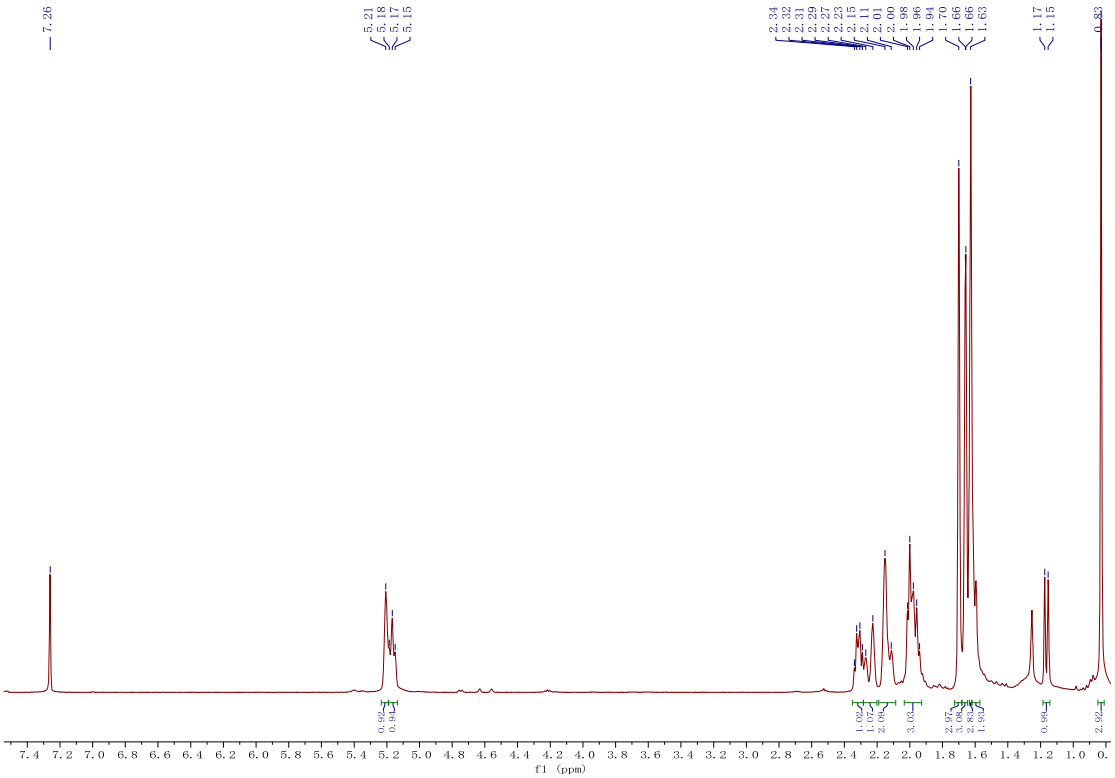

Fig. S17. ^{1}H NMR spectrum of 7 in $CDCl_3$ at 400 MHz

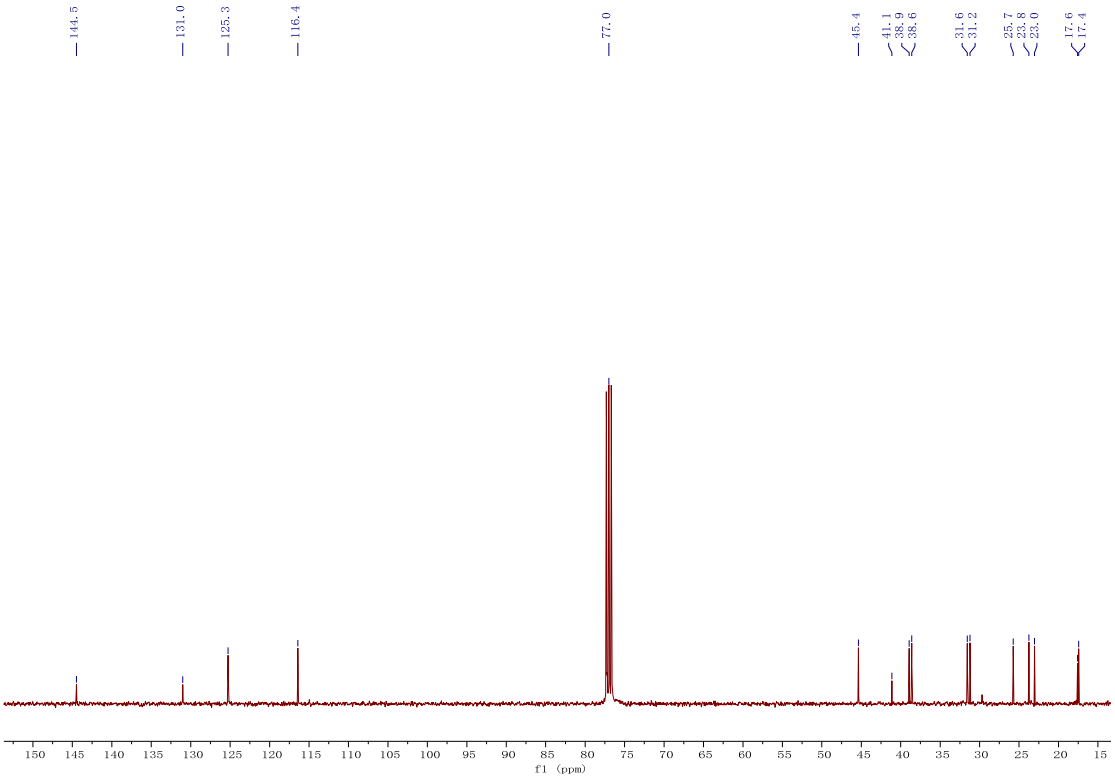

Fig. S18. ^{13}C NMR spectrum of 7 in $CDCl_3$ at 100 MHz

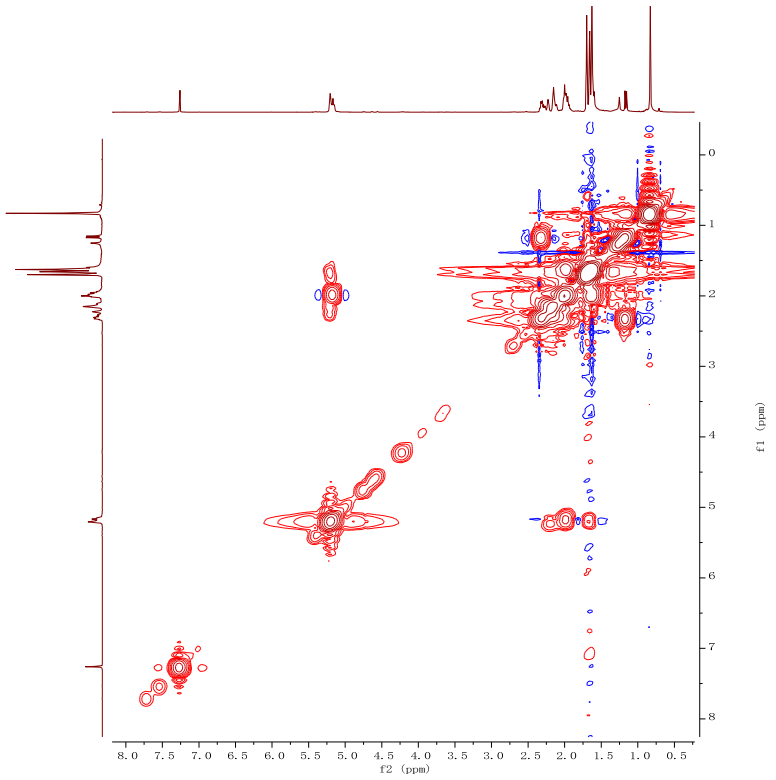

Fig. S19. ^{1}H-^{1}H COSY spectrum of 7 in $CDCl_3$ at 400 MHz

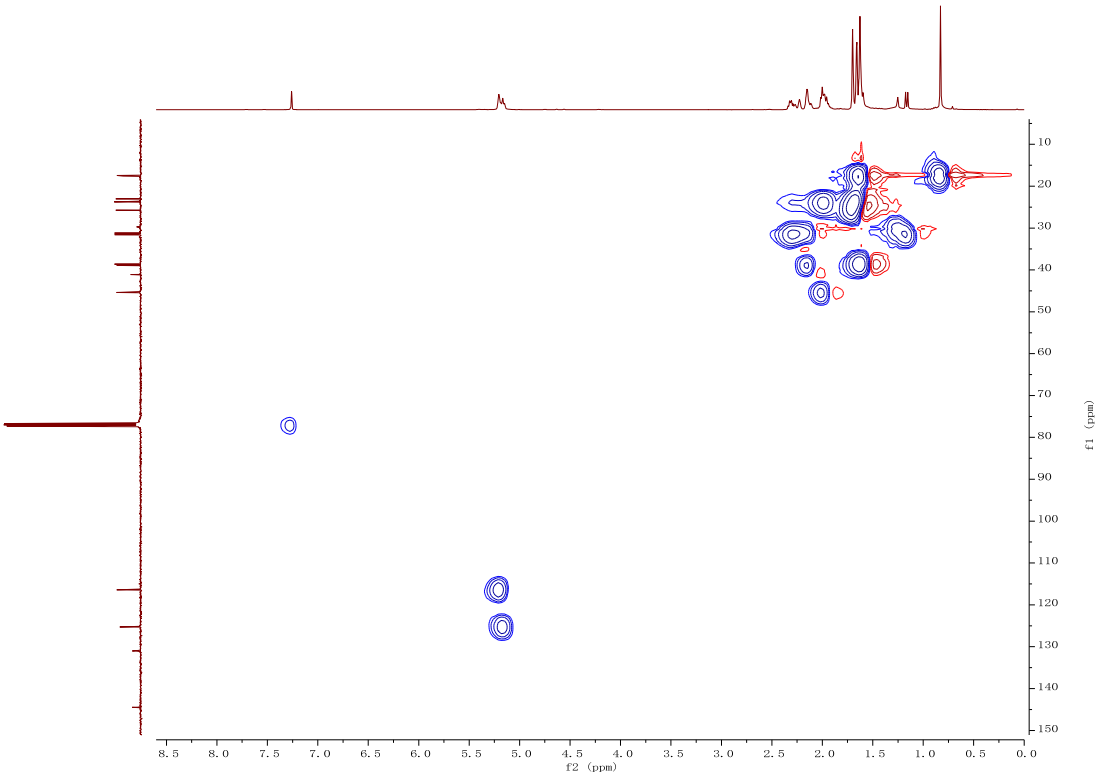

Fig. S20. HSQC spectrum of 7 in $CDCl_3$ at 400 MHz

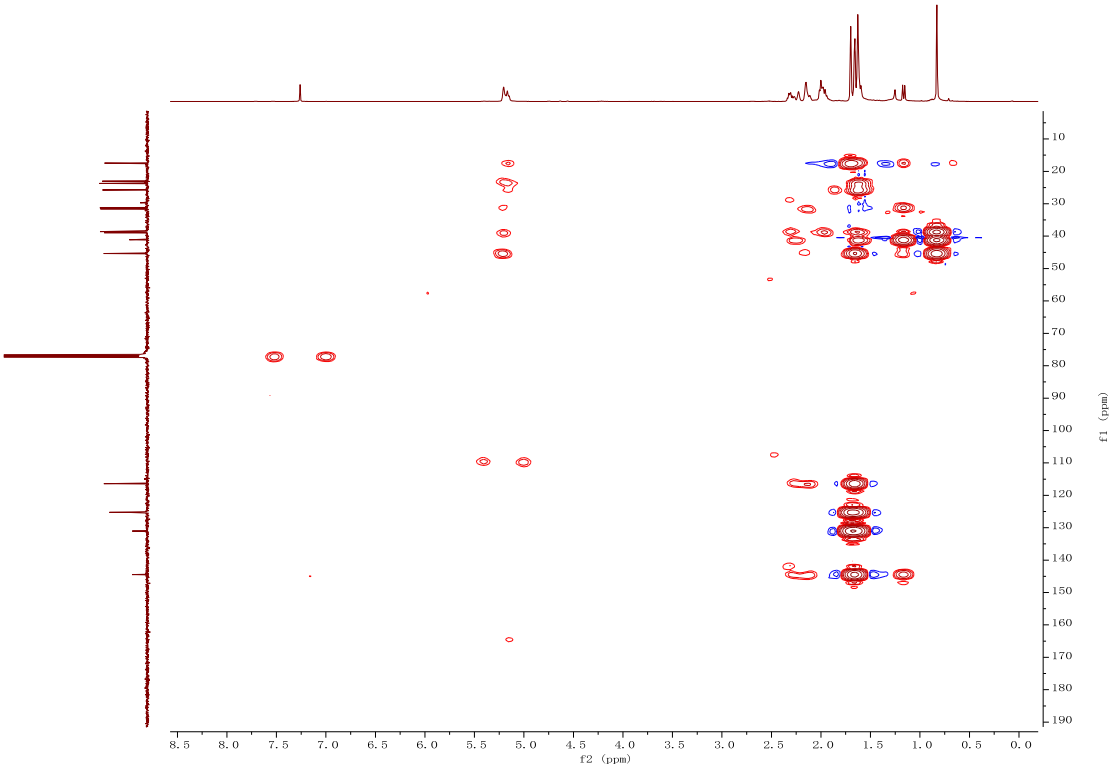

Fig. S21. HMBC spectrum of 7 in $CDCl_3$ at 400 MHz

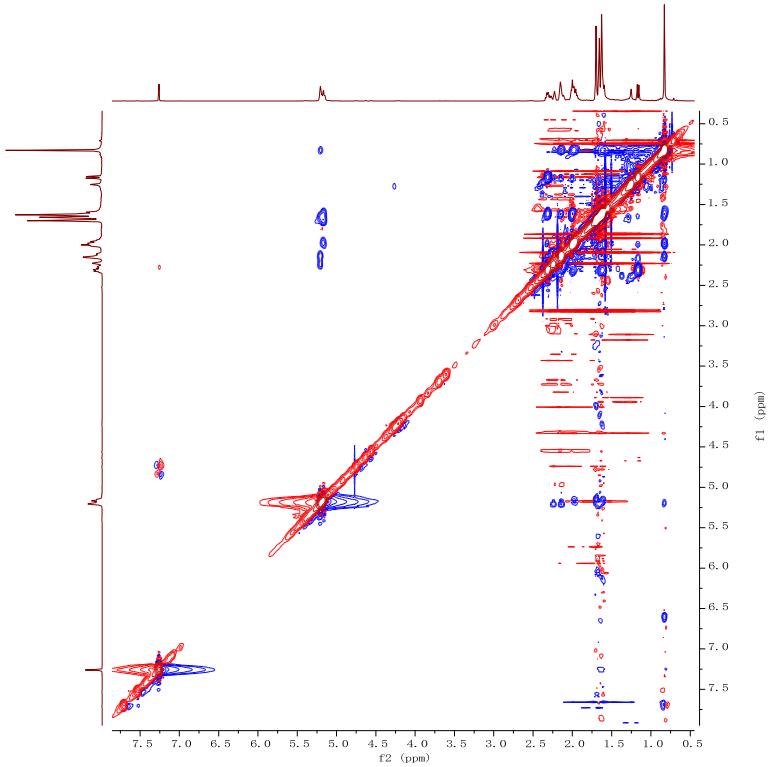

Fig. S22. NOESY spectrum of 7 in $CDCl_3$ at 600 MHz

Single Mass Analysis
Tolerance = 5.0 PPM / DBE: min = -1.5, max = 50.0
Element prediction: Off
Number of isotope peaks used for i-FIT = 2

Monoisotopic Mass, Even Electron Ions
290 formula(e) evaluated with 1 results within limits (all results (up to 1000) for each mass)
Elements Used:
C: 0-500 H: 0-1000 N: 0-6 O: 0-500 Na: 0-1

2082-1
20210816003 279 (2.244)

1: TOF MS ES+
4.12e+004

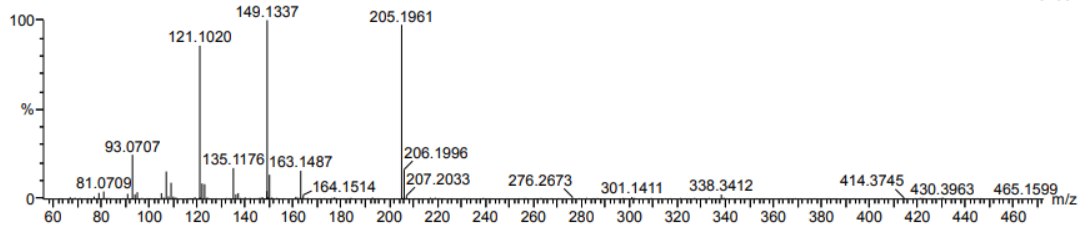

Minimum:				-1.5			
Maximum:		5.0	5.0	50.0			
Mass	Calc. Mass	mDa	PPM	DBE	i-FIT	Conf(%)	Formula
205.1961	205.1956	0.5	2.4	3.5	115.6	n/a	C15 H25

Fig. S23. HR-ESI-MS spectrum of 8

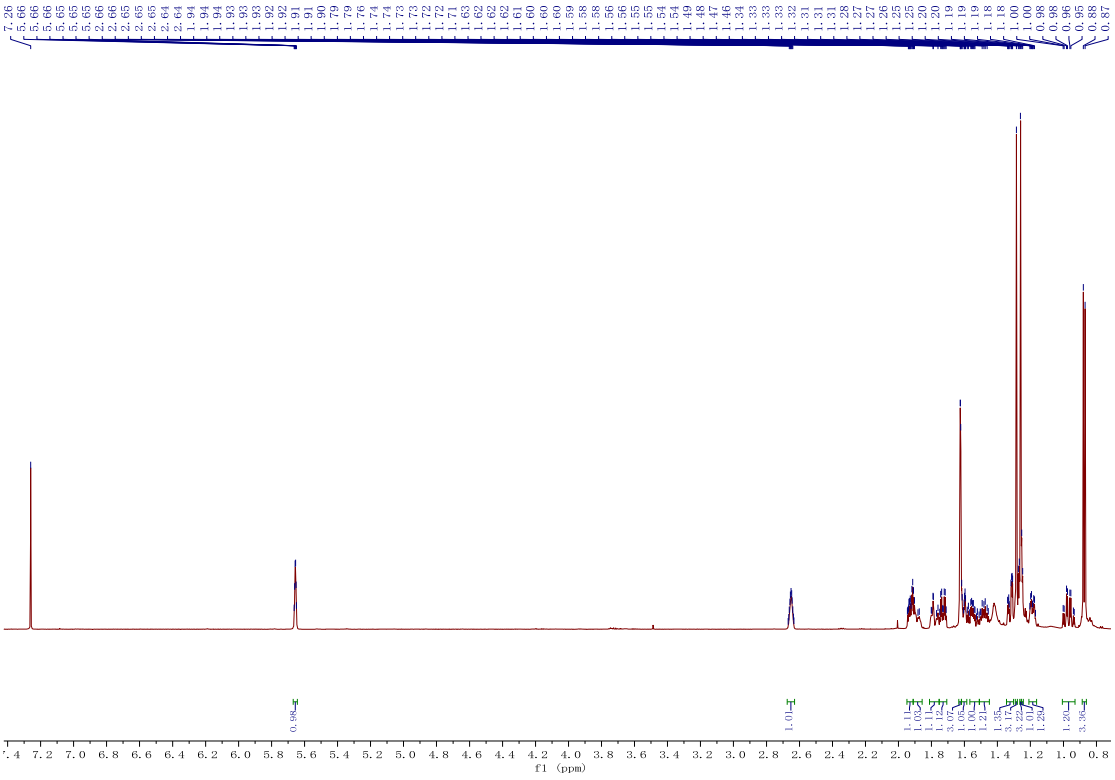

Fig. S24. ^{1}H NMR spectrum of 8 in $CDCl_3$ at 600 MHz

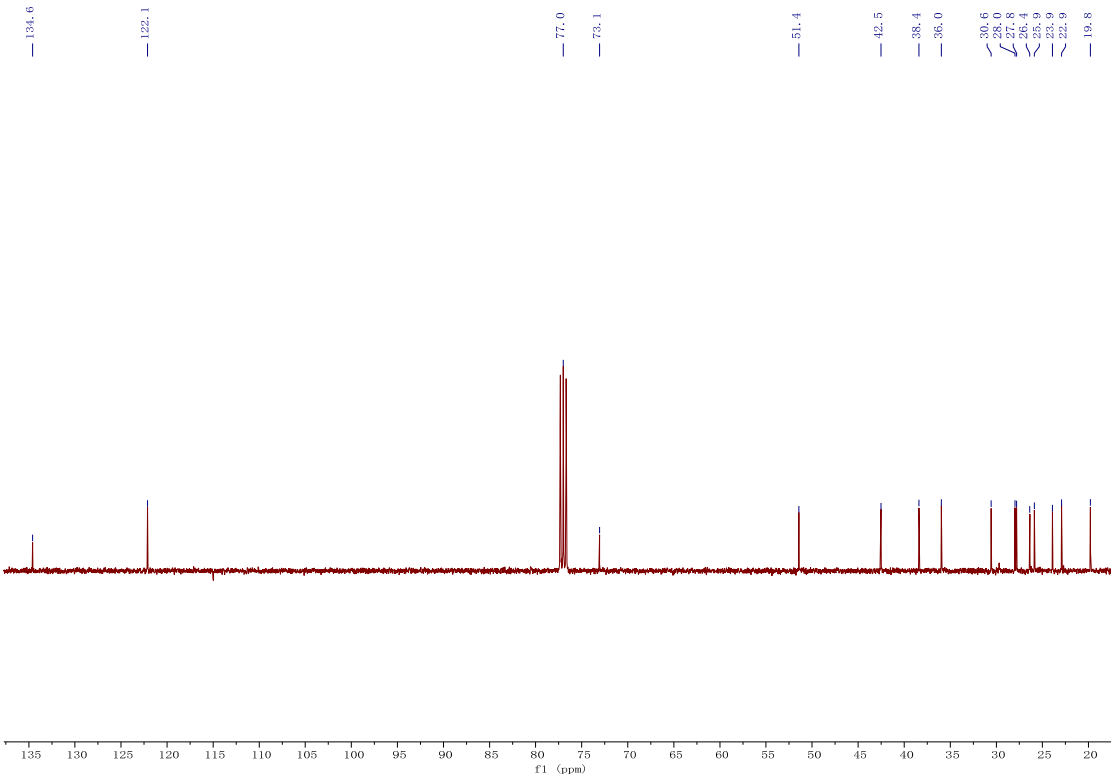

Fig. S25. ^{13}C NMR spectrum of 8 in $CDCl_3$ at 100 MHz

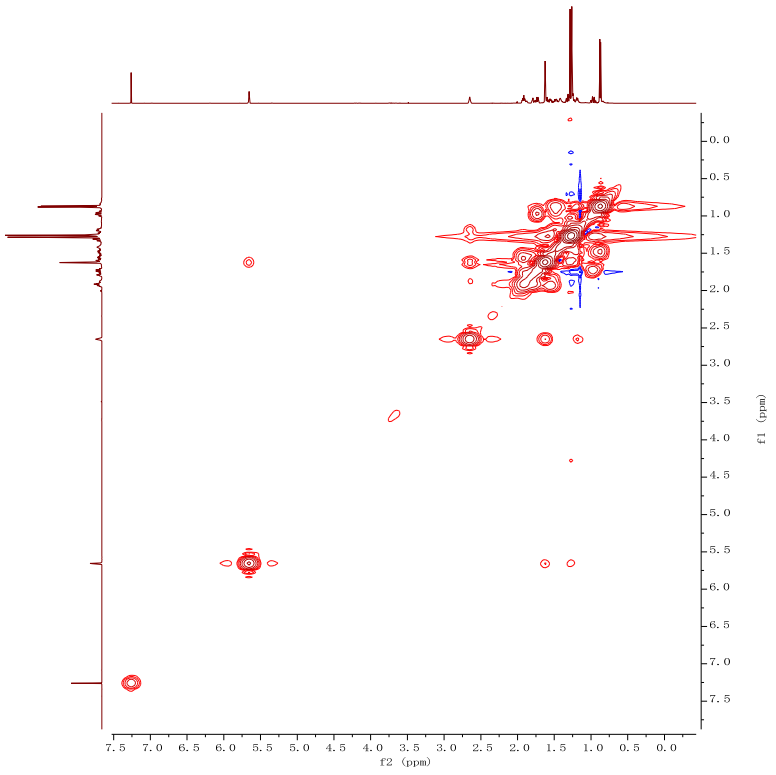

Fig. S26. ^{1}H-^{1}H COSY spectrum of 8 in $CDCl_3$ at 400 MHz

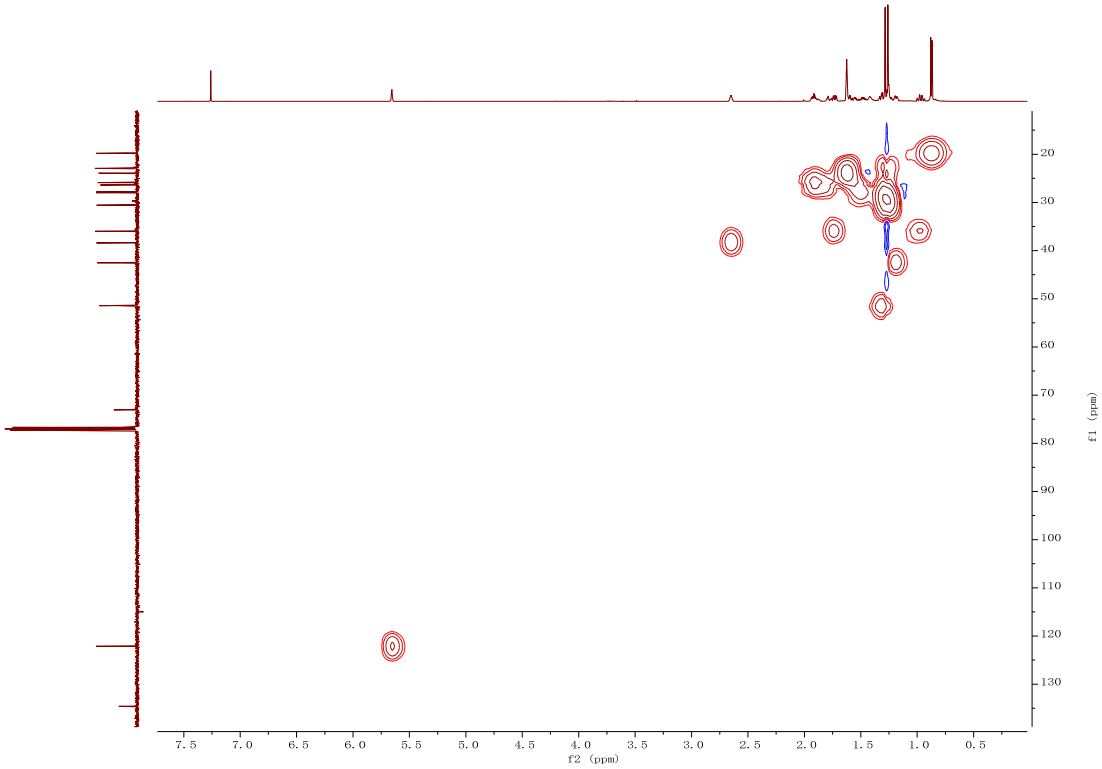

Fig. S27. HSQC spectrum of 8 in $CDCl_3$ at 400 MHz

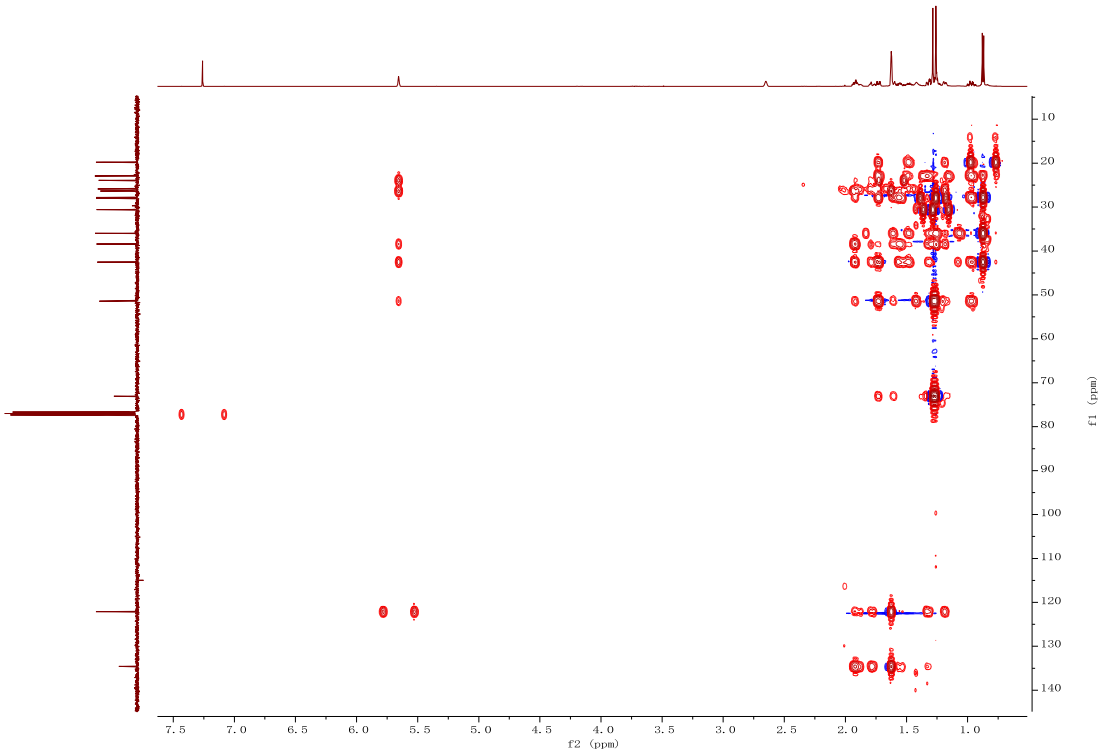

Fig. S28. HMBC spectrum of 8 in $CDCl_3$ at 600 MHz

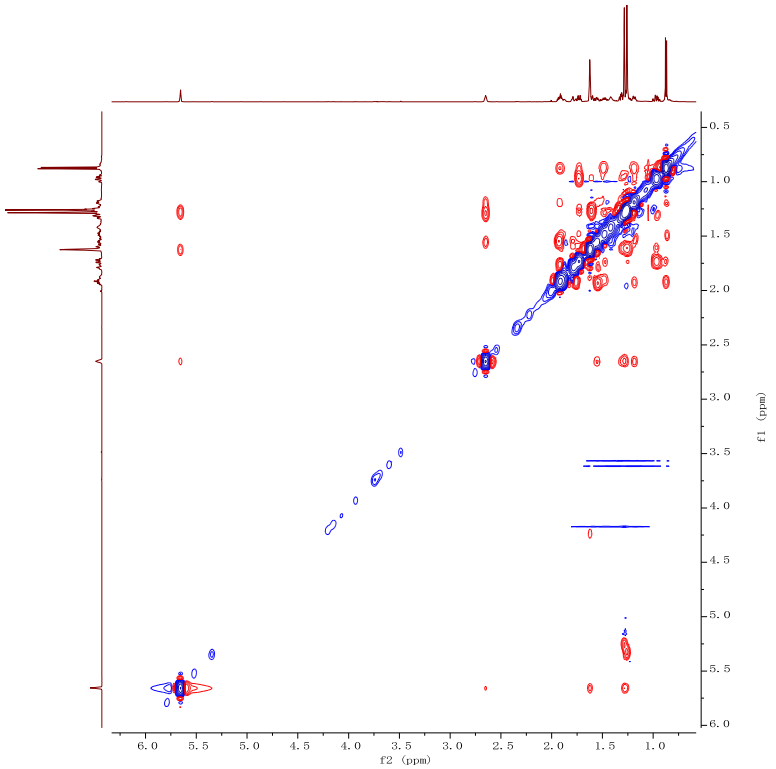

Fig. S29. NOESY spectrum of 8 in $CDCl_3$ at 600 MHz

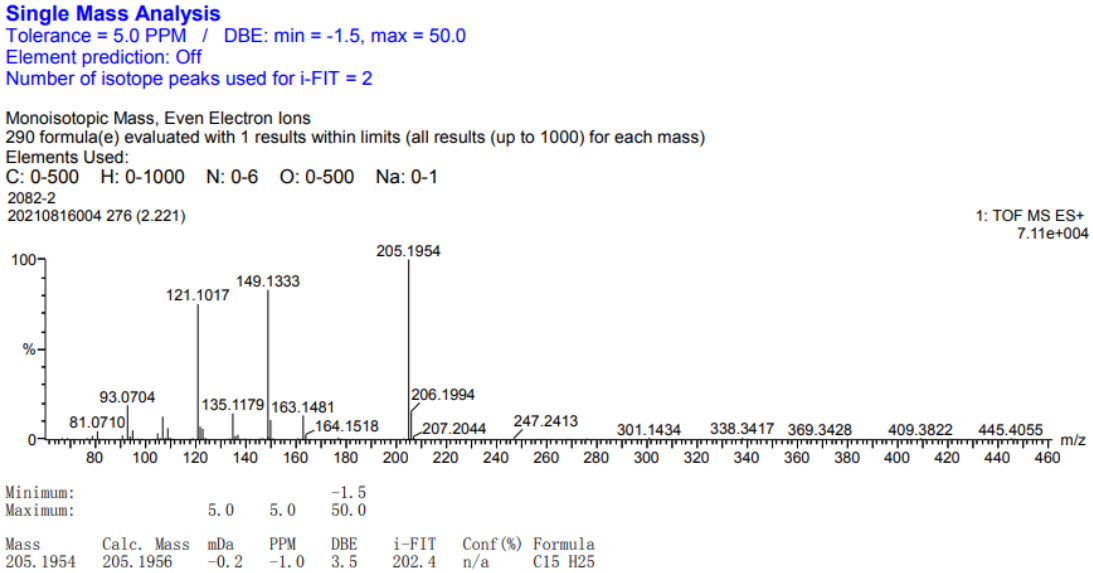

Fig. S30. HR-ESI-MS spectrum of 9

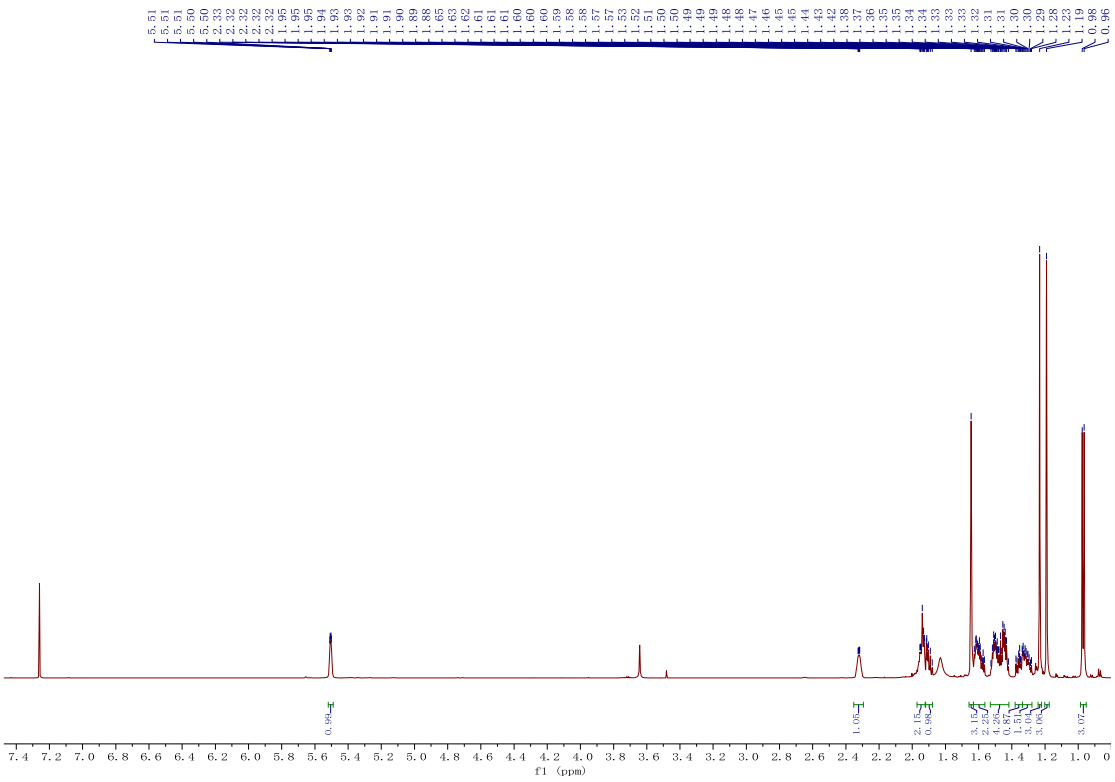

Fig. S31. ^{1}H NMR spectrum of 9 in $CDCl_3$ at 600 MHz

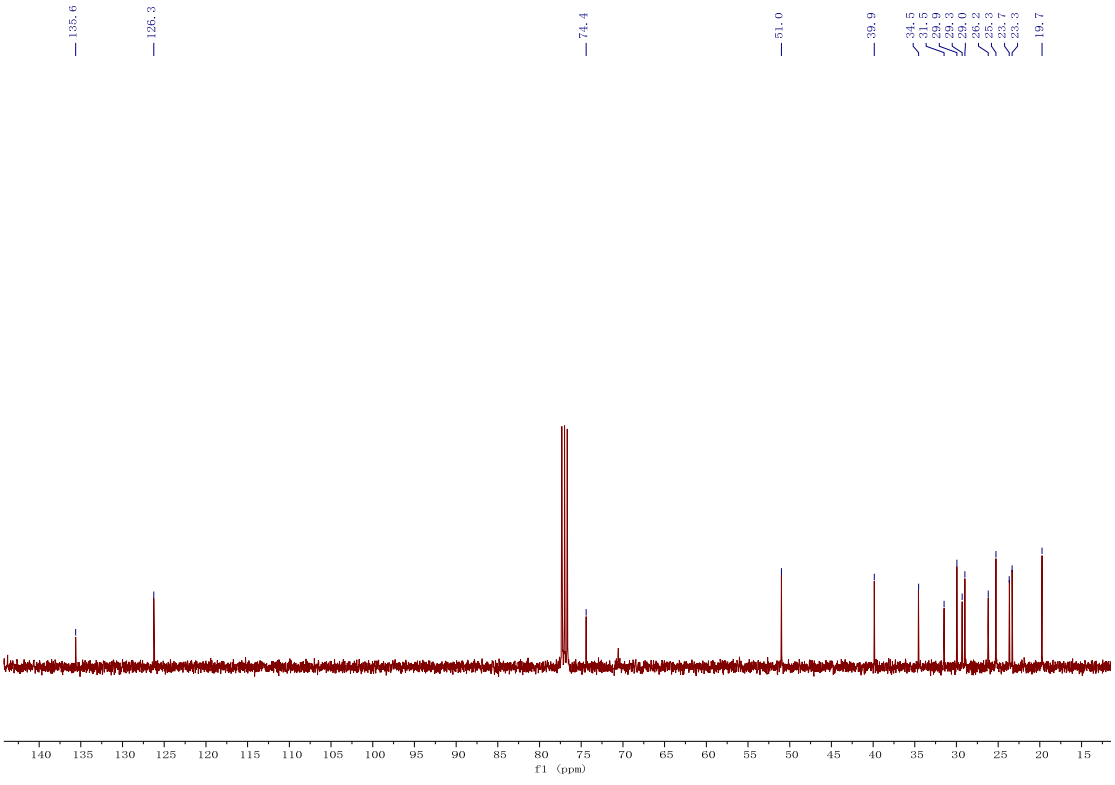

Fig. S32. ^{13}C NMR spectrum of 9 in $CDCl_3$ at 100 MHz

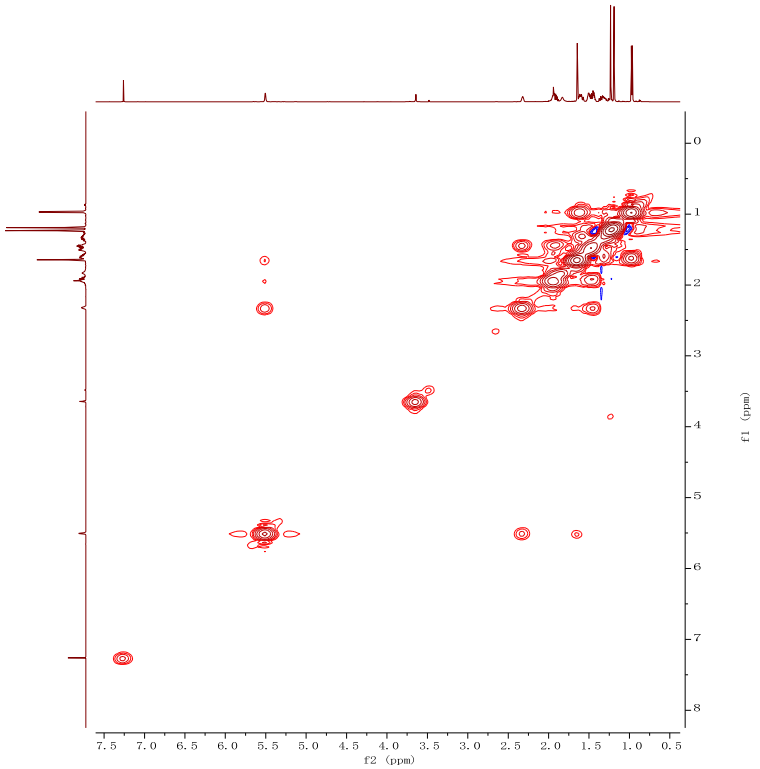

Fig. S33. ^{1}H-^{1}H COSY spectrum of 9 in $CDCl_3$ at 400 MHz

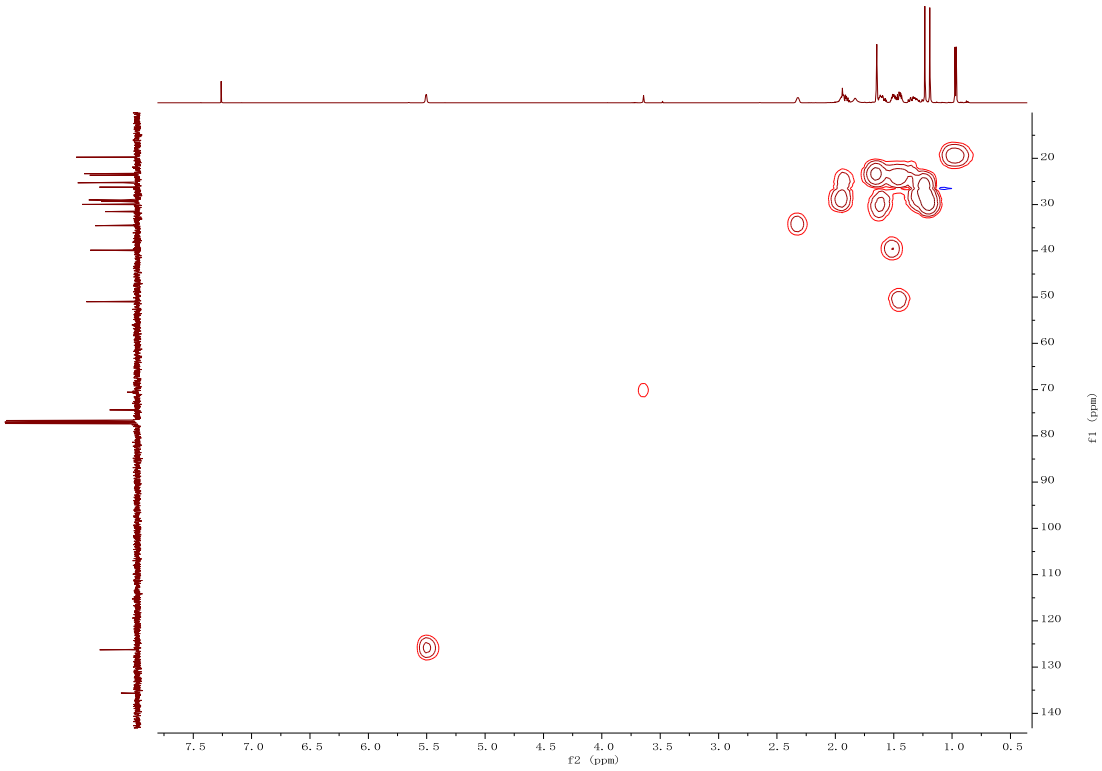

Fig. S34. HSQC spectrum of 9 in $CDCl_3$ at 400 MHz

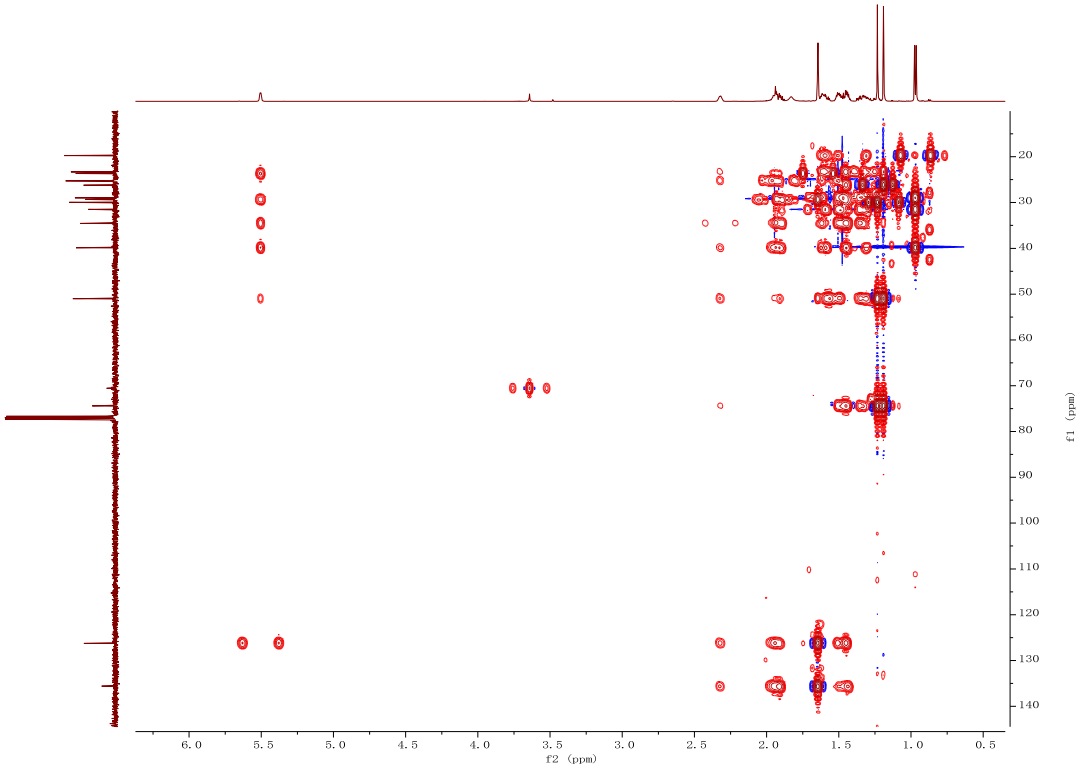

Fig. S35. HMBC spectrum of 9 in $CDCl_3$ at 600 MHz

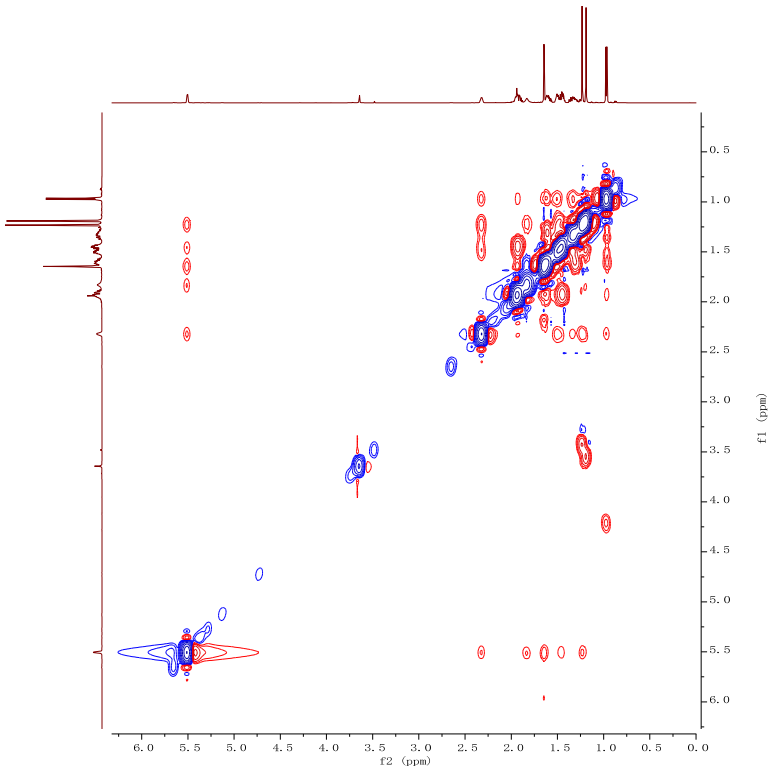

Fig. S36. NOESY spectrum of 9 in $CDCl_3$ at 600 MHz

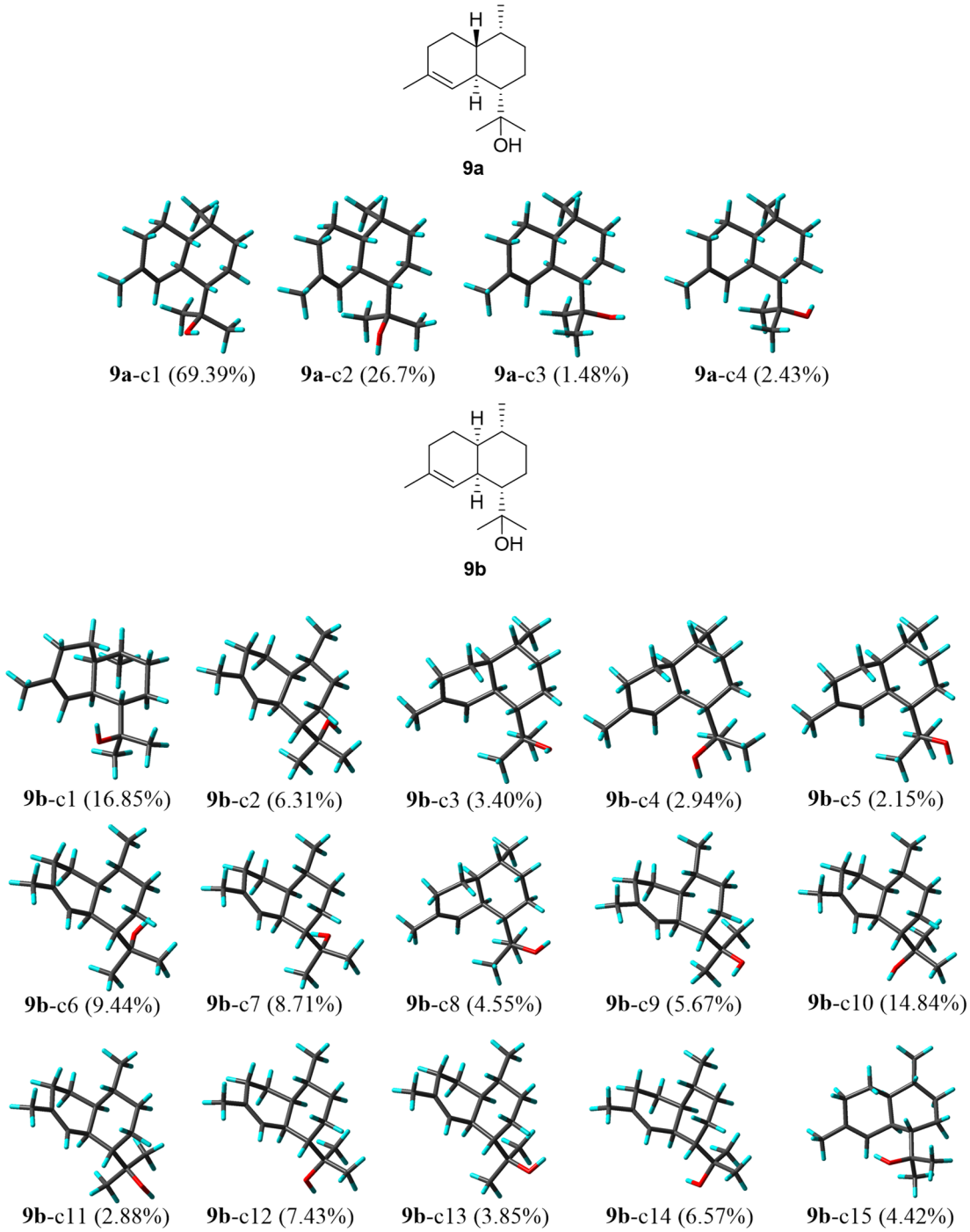

Fig. S37. Stable conformers of 9a and 9b used in ^{13}C NMR calculation

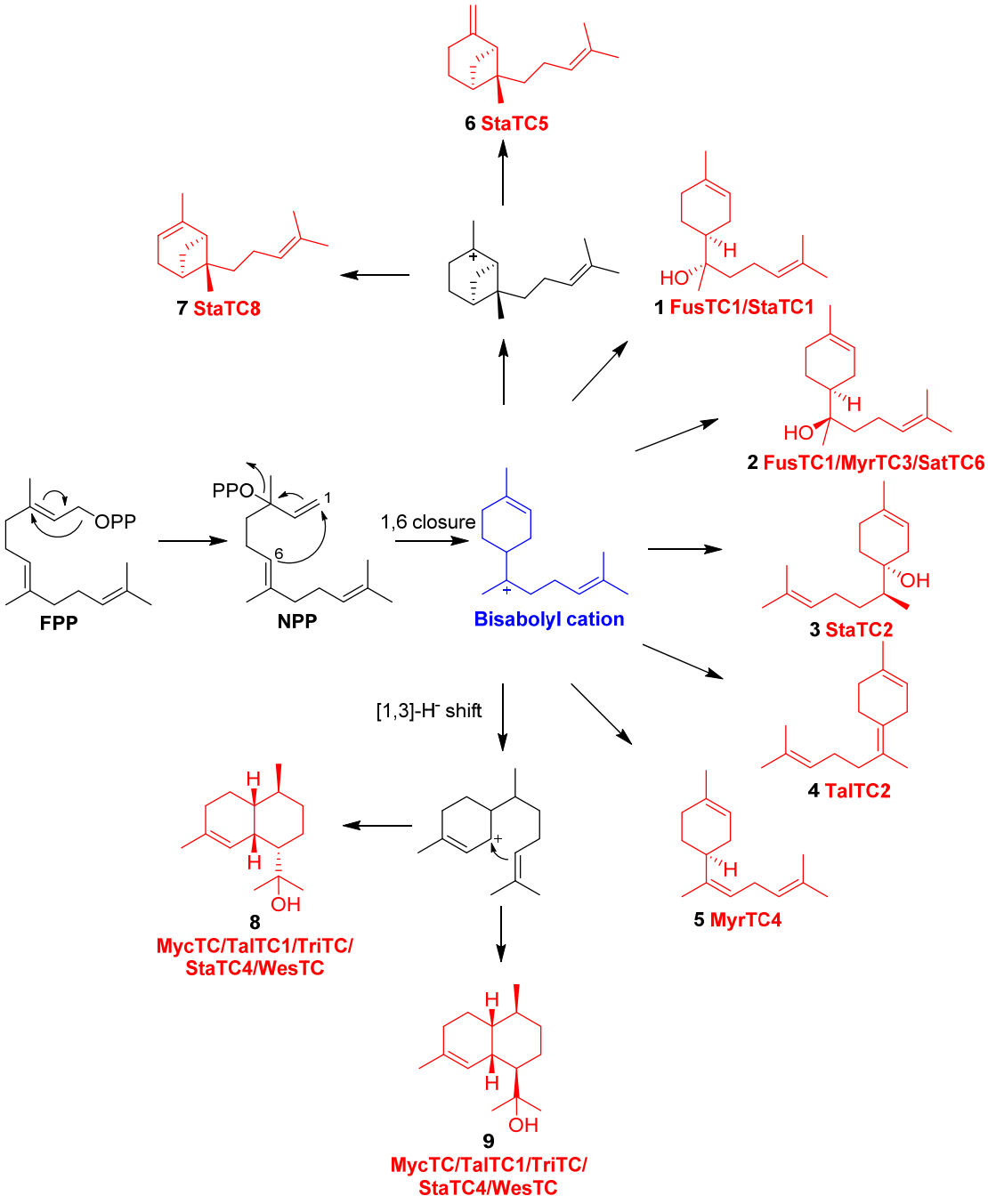

Fig. S38. Proposed cyclization mechanism of compounds 1–9

Supplementary References

1. N. Makita, Y. Hoshino and H. Yamamoto, Asymmetric epoxidation of homoallylic alcohols and application in a concise total synthesis of (–)-α-bisabolol and (–)-8-*epi*-α-bisabolol, *Angew. Chem. Int. Ed.*, 2003, **115**, 971–973.
2. O. Günther, G. Wolfgang, N. Regula and D. François, The absolute configuration of β-bisabolol, *Helv. Chim. Acta*, 1986, **69**, 698–703.
3. G. Fráter and U. Müller, Synthesis of (+)-(4*S*, 8*R*)-8-*epi*- and (−)-(4*R*, 8*S*)-4-*epi*-β-bisabolol, *Helv. Chim. Acta*, 1989, **72**, 653–658.
4. L. Anastasia, Y. Dumond and E. Negishi, Stereoselective synthesis of exocyclic alkenes by Cu-catalyzed allylmagnesiation, Pd-catalyzed alkylation, and Ru-catalyzed ring-closing metathesis: Highly stereoselective synthesis of (*Z*)- and (*E*)-γ-bisabolenes, *Euro. J. Org. Chem.*, 2001, **2001**, 3039–3043.
5. D. François and O. Günther, Syntheses and absolute configuration of (*E*)- and (*Z*)-α-bisabolenes, *Helv. Chim. Acta*, 1979, **62**, 369–377.
6. H. C. Lin, Y. H. Chooi, S. Dhingra, W. Xu, A. M. Calvo and Y. Tang, The fumagillin biosynthetic gene cluster in *Aspergillus fumigatus* encodes a cryptic terpene cyclase involved in the formation of β-*trans*-bergamotene, *J. Am. Chem. Soc.*, 2013, **135**, 4616–4619.
7. D. E. Cane, D. B. Mcilwaine and J. S. Oliver, Absolute configuration of (–)-β-*trans*-bergamotene, *J. Am. Chem. Soc.*, 1990, **112**, 1285–1286.
8. C. Chapuis, M. Barthe, B. L. Muller and K. H. Schulte-Eke, Preparation and absolute configuration of (–)-(*E*)-α-*trans*-bergamotenone, *Helv. Chim. Acta*, 1998, **81**, 153–162.
9. K. S. Ngo and G. D. Brown, Synthesis of amorphane and cadinane sesquiterpenes from *Fabiana imbricata*, *Tetrahedron*, 1999, **55**, 15099–15108.
10. J. F. M., G, W. Trucks, H. B. Schlegel, G. E. Scuseria, M. A. Robb, J. R. Cheeseman, G. Scalmani, V. Barone, B. Mennucci and G. A. Petersson, Gaussian 09 (Revision A. 1), Gaussian Inc., Wallingford, CT, 2009.
11. N. Grimblat, M. M. Zanardi and A. M. Sarotti, Beyond DP4: an improved probability for the stereochemical assignment of isomeric compounds using quantum chemical calculations of NMR shifts, *J. Org. Chem.*, 2015, **80**, 12526.